ผลของฟิลด์อ็อฟวิวต่อปริมาณรังสีของเครื่องถ่ายภาพรังสีส่วนตัดอาศัยคอมพิวเตอร์ ชนิดลำรังสีรูปกรวย: ศึกษาในหุ่นจำลอง

นางสาววรางคณา วีระวานิช

จุฬาลงกรณ์มหาวิทยาลัย
Chulalongkorn University

วิทยานิพนธ์นี้เป็นส่วนหนึ่งของการศึกษาตามหลักสูตรปริญญาวิทยาศาสตรมหาบัณฑิต
สาขาวิชาฉายาเวชศาสตร์ ภาควิชารังสีวิทยา
คณะแพทยศาสตร์ จุฬาลงกรณ์มหาวิทยาลัย
ปีการศึกษา 2556
ลิขสิทธิ์ของจุฬาลงกรณ์มหาวิทยาลัย

บทคัดย่อและแฟ้มข้อมูลฉบับเต็มของวิทยานิพนธ์ตั้งแต่ปีการศึกษา 2554 ที่ให้บริการในคลังปัญญาจุฬาฯ (CUIR)
เป็นแฟ้มข้อมูลของนิสิตเจ้าของวิทยานิพนธ์ ที่ส่งผ่านทางบัณฑิตวิทยาลัย
The abstract and full text of theses from the academic year 2011 in Chulalongkorn University Intellectual Repository (CUIR)
are the thesis authors' files submitted through the University Graduate School.

EFFECT OF FIELD OF VIEWS ON CONE BEAM COMPUTED TOMOGRAPHY RADIATION DOSE: PHANTOM STUDY

Miss Warangkana Weerawanich

จุฬาลงกรณ์มหาวิทยาลัย
Chulalongkorn University

A Thesis Submitted in Partial Fulfillment of the Requirements
for the Degree of Master of Science Program in Medical Imaging
Department of Radiology
Faculty of Medicine
Chulalongkorn University
Academic Year 2013

Copyright of Chulalongkorn University

Thesis Title	EFFECT OF FIELD OF VIEWS ON CONE BEAM COMPUTED TOMOGRAPHY RADIATION DOSE: PHANTOM STUDY
By	Miss Warangkana Weerawanich
Field of Study	Medical Imaging
Thesis Advisor	Associate Professor Anchali Krisanachinda, Ph.D.

Accepted by the Faculty of Medicine, Chulalongkorn University in Partial Fulfillment of the Requirements for the Master's Degree

.....Dean of the Faculty of Medicine

(Associate Professor Sophon Napathorn, M.D.)

THESIS COMMITTEE

.....Chairman

(Associate Professor Sukalaya Lerdlum, M.D.)

.....Thesis Advisor

(Associate Professor Anchali Krisanachinda, Ph.D.)

.....External Examiner

(Professor Franco Milano, Ph.D.)

จุฬาลงกรณ์มหาวิทยาลัย
Chulalongkorn University

วรางคณา วีระวานิช : ผลของฟิลด์อ็อฟวิวต่อปริมาณรังสีของเครื่องถ่ายภาพรังสีส่วนตัดอาศัยคอมพิวเตอร์ ชนิดลำรังสีรูปกรวย: ศึกษาในหุ่นจำลอง. (EFFECT OF FIELD OF VIEWS ON CONE BEAM COMPUTED TOMOGRAPHY RADIATION DOSE: PHANTOM STUDY) อ.ที่ปรึกษาวิทยานิพนธ์หลัก: รศ. ดร. อัญชลี กฤษณจินดา, 78 หน้า.

ในปัจจุบันเครื่องถ่ายภาพรังสีส่วนตัดอาศัยคอมพิวเตอร์ชนิดลำรังสีรูปกรวยมีหลายแบบ ซึ่งแต่ละแบบมีฟิลด์อ็อฟวิวหลายขนาดให้เลือกใช้ตามความเหมาะสม การเลือกใช้ฟิลด์อ็อฟวิวและจำนวนครั้งในการสแกน ขึ้นอยู่กับการนำไปใช้ทางคลินิก และหลักการลดปริมาณรังสีจนเป็นที่ยอมรับ (ALARA) วัตถุประสงค์ของการศึกษานี้เพื่อศึกษาผลของจำนวนครั้งที่สแกนและขนาดฟิลด์อ็อฟวิวได้แก่ขนาดใหญ่ 1ครั้ง ขนาดกลาง 1ครั้งและขนาดเล็กหลายครั้งต่อปริมาณรังสีจากเครื่องถ่ายภาพรังสีส่วนตัดอาศัยคอมพิวเตอร์ชนิดลำรังสีรูปกรวย 3เครื่อง โดยศึกษาในหุ่นจำลอง

กระบวนการคือ ศึกษาปริมาณรังสีในปริมาตรเป็นค่าซีทีดีไอวอลลุ่ม (มิลลิเกรย์) ปริมาณรังสีตามความยาวของการสแกน (มิลลิเกรย์.เซนติเมตร) และปริมาณรังสียังผล (ไมโครซีเวิร์ต) ในหุ่นจำลอง จากเครื่องถ่ายภาพรังสีผลิตภัณฑ์ 3D Accuitomo 170 ส่วนเครื่องถ่ายภาพรังสีผลิตภัณฑ์ Kodak9000 3D และ Kodak9500 CB 3D จะศึกษาปริมาณรังสีกับพื้นที่ (มิลลิเกรย์.ตารางเซนติเมตร) สำหรับการสแกนฟิลด์อ็อฟวิวขนาดเล็ก 2 หรือ 3 ครั้ง ปริมาณรังสีจะได้จากการคำนวณ

ค่าซีทีดีไอวอลลุ่มในฟิลด์อ็อฟวิวที่มีขนาดเล็กกว่า 16เซนติเมตร (เส้นผ่านศูนย์กลางของหุ่นจำลองพีเอ็มเอ็มเอ) มีความไม่แม่นยำ ดังนั้นในเครื่อง 3D Accuitomo 170 จึงรายงานปริมาณรังสีที่ได้จากฟิลด์อ็อฟวิวขนาด 17x5 และ 17x12 ตารางเซนติเมตร โดยค่าซีทีดีไอวอลลุ่มปริมาณรังสีตามความยาวสแกน ปริมาณรังสียังผล มีค่าเท่ากับ 7.7, 38.5, 88.55 และ 6.4, 76.8, 176.64 ตามลำดับ สำหรับเครื่อง Kodak9000 3D และ Kodak9500 CB 3D ค่าปริมาณรังสีกับพื้นที่ของฟิลด์อ็อฟวิวขนาด 5x3.7 ตารางเซนติเมตร, 9.3x5x3.7 ลูกบาศก์เซนติเมตร, 9.3x7.4x3.7 ลูกบาศก์เซนติเมตร, 15x9 ตารางเซนติเมตร และ 20.6x18 ตารางเซนติเมตร มีค่าเท่ากับ 131, 261, 392, 211 และ 502 มิลลิเกรย์.ตารางเซนติเมตร ตามลำดับ และปริมาณรังสีกับพื้นที่ ที่ได้จากการสแกนฟิลด์อ็อฟวิวขนาด 5x3.7 ตารางเซนติเมตร สองและสามครั้ง มีค่าเท่ากับ 262 และ 393 มิลลิเกรย์.ตารางเซนติเมตร ตามลำดับ จากผลการศึกษาพบว่า ปริมาณรังสีเพิ่มขึ้น เมื่อขนาดฟิลด์อ็อฟวิวใหญ่ขึ้นและจำนวนครั้งที่สแกนเพิ่มขึ้น

ภาควิชา รังสีวิทยา ลายมือชื่อนิสิต .....

สาขาวิชา ฉายาเวชศาสตร์ ลายมือชื่อ อ.ที่ปรึกษาวิทยานิพนธ์หลัก .....

ปีการศึกษา 2556

5574157030 : MAJOR MEDICAL IMAGING
KEYWORDS: CONE BEAM COMPUTED TOMOGRAPHY / CBCT / DOSIMETRY / MULTI-SMALL FIELD OF VIEWS / DAP

WARANGKANA WEERAWANICH: EFFECT OF FIELD OF VIEWS ON CONE BEAM COMPUTED TOMOGRAPHY RADIATION DOSE: PHANTOM STUDY. ADVISOR: ASSOC. PROF. ANCHALI KRISANACHINDA, Ph.D., 78 pp.

Currently, there are many cone beam computed tomography (CBCT) devices with various field of views (FOVs). Thus the selection of proper FOVs and number of scans should be considered based on clinical applications and ALARA principle. The purpose of this study is to study the effect on number of scans and field of views such as large, medium and multi-small, on the radiation dose from CBCT systems in phantom study.

Radiation dose from 3 CBCT devices were recorded by using RANDO phantom. For 3D Accuitomo170, C_vol (mGy), DLP (mGy.cm) and the effective dose (E:μSv) were determined. For Kodak devices, DAP (mGy.cm^2) was recorded. In two or three scans of small FOV, E and DAP were obtained.

Inaccuracy in C_vol verification is obtained when FOVs are less than 16cm (PMMA phantom diameter). For 3D Accuitomo 170, the radiation dose reported in C_vol (mGy), DLP (mGy.cm) and E (μSv) of FOV 17x5 and 17x12cm^2 were 7.7, 38.5, 88.55 and 6.4, 76.8, 176.64 respectively. For Kodak9000 3D and Kodak9500 CB 3D, FOV 5x3.7cm^2, 9.3x5x3.7cm^3, 9.3x7.4x3.7cm^3, 15x9cm^2 and 20.6x18cm^2, DAP values were 131, 261, 392, 211 and 502 mGy.cm^2 respectively. Two and three scans of FOV 5x3.7cm^2 were 262 and 393 mGy.cm^2 respectively. In conclusion, the radiation dose is higher when the FOVs and number of scans increase.

จุฬาลงกรณ์มหาวิทยาลัย
Chulalongkorn University

Department: Radiology Student's Signature .....

Field of Study: Medical Imaging Advisor's Signature .....

Academic Year: 2013

ACKNOWLEDGEMENTS

I would like to deeply appreciate and express my gratitude to Associate Professor Anchali Krisanachinda, Ph.D., my advisor, for invaluable advice, supervision, constructive comments and English language proof in this research.

I would like to thank Associate Professor Sukalaya Lerdlum, M.D., Chairperson of thesis defense and Professor Franco Milano, Ph.D., External examiner for their kind suggestion and constructive comments in this research.

I would like to thank Associate Professor Sivalee Suriyapee, M.Eng., for teaching in Medical Imaging, comments in this research and kind support on equipment and RANDO phantom.

I would like to thank Mrs. Petcharleeya Suwanpradit, M.Sc., and staff of Department of Radiology, King Chulalongkorn Memorial Hospital for their kind support in equipment for this research.

I would like to thank Mr. Kittiwat Khamwan, Ph.D., for his help and comments in this research.

I would like to thank Mrs.Weeranuch Kitsukjit, Consultant in statistical analysis.

I would like to thank all teachers, lecturers and staff in Master of Science Program for their unlimited teaching in Medical Imaging.

I would like to thank Dean of Faculty of Dentistry, Mahidol University for his permission to use cone beam computed tomography system.

I would like to thank Assistant Professor Suchaya Damrongsri, Ph.D., and all lecturers in Department of Oral and Maxillofacial Radiology, Faculty of Dentistry, Mahidol University for their kind support with sympathy.

Finally I would like to thank my family for caring, encouraging and sympathy.

CONTENTS

Page

THAI ABSTRACT iv
ENGLISH ABSTRACT v
ACKNOWLEDGEMENTS vi
CONTENTS vii
LIST OF TABLES xi
LIST OF FIGURES xiii
LIST OF ABBREVIATIONS xvi
CHAPTER I INTRODUCTION 1
1.1. Background and Rationale 1
1.2. Objective 2
CHAPTER II REVIEW OF RELATED LITERATURE 3
2.1. Theory 3
2.1.1. Principle of Cone Beam Computed Tomography 3
2.1.2. Image acquisition 4
2.1.2.1. CBCT system: Image acquisition 4
2.1.2.2. Image detection system [2, 8] 5
2.1.2.3. Image reconstruction [1, 2] 6
2.1.2.4. Image display [1, 2] 7
2.1.3. Quantities for CT dosimetry 7
2.1.3.1. CT air kerma index 7
2.1.3.2. Effective dose 9
2.1.3.3. Air kerma area product 9
2.2. Review of Related Literature 9
CHAPTER III RESEARCH METHODOLOGY 12
3.1. Research Design 12
3.2. Keywords 12
3.3. Research Design Model 13

จุฬาลงกรณ์มหาวิทยาลัย
CHULALONGKORN UNIVERSITY

Page

3.4. Conceptual Framework 14
3.5. Research Question 14
3.6. Material 14
3.6.1. CBCT devices 14
3.6.1.1. 3D Accuitomo 170 (J. MORITA Mfg. Corp., Kyoto, Japan) 15
3.6.1.2. Kodak 9000 3D Extraoral Imaging System (Carestream health, Inc., New York, USA) 16
3.6.1.3. Kodak 9500 Cone Beam 3D System (Carestream health, Inc., New York, USA) 17
3.6.2. QC material 18
3.6.2.1. Unfors Raysafe Xi dosimeter 18
3.6.2.2. PMMA 16 cm diameter cylindrical phantom 19
3.6.2.3. DAP meter: PTW Freiburg Model Diamentor E 20
3.6.2.4. CATPHAN phantom® 600 20
3.6.2.5. QC kit of 3D Accuitomo 170 20
3.6.3. RANDO phantom: head and neck part 21
3.7. Methods 21
3.8. Data Analysis 24
3.9. Sample Size Determination 24
3.10. Statistical Analysis 24
3.11. Outcome Measurement 24
3.12. Expected Benefit 25
3.13. Ethical Considerations 25
CHAPTER IV RESULTS 26
4.1. Quality control of the CBCT systems 26
4.2. Dose measurement 26
4.2.1. Radiation doses (C_{VOL}, DLP, E) of 3D Accuitomo 170 27
4.2.2. Radiation dose, DAP, of Kodak9000 3D and Kodak9500 Cone Beam 3D. 28

CHULALONGKORN UNIVERSITY

Page

CHAPTER V DISCUSSION AND CONCLUSION 29
5.1. Discussion 29
5.2. Conclusion 31
REFERENCES 32
APPENDICES 34
Appendix A: Data record form 35
1. Data record form of 3D Accuitomo 170 35
2. Data record form of Kodak 9000 3D and Kodak 9500 CB 3D 35
Appendix B: Quality control of the CBCT scanner – 3D Accuitomo170 FPD XYZ Slice View Tomograph 36
1. kVp accuracy 36
2. mAs linearity 37
3. $C_{a,100}$ 39
4. CT dose index 40
5. Spatial resolution test 44
6. Noise, Uniformity/Grayscale and contrast resolution test 45
7. Artifact test 46
8. Patient position test 47
Appendix C: Quality control of the CBCT scanner – Kodak 9000 3D 49
1. kVp accuracy 49
2. mAs linearity 50
3. $C_{a,100}$ 52
4. Dose area product 53
5. Rotative arm axis 55
6. Spatial linearity 56
7. MTF measurement 56
Appendix D: Quality control of the CBCT scanner – Kodak 9500 Cone Beam 3D 58
1. kVp accuracy 58

CHULALONGKORN UNIVERSITY

Page

2. mAs linearity 61
3. $C_{a,100}$ 63
4. Dose area product 63
5. Rotative arm axis 65
6. Circular symmetry and spatial linearity 66
7. MTF measurement 69
8. High resolution measurement 71
9. CT number accuracy, noise, uniformity and image artifact 72
10. CT number linearity 75

VITA 78

จุฬาลงกรณ์มหาวิทยาลัย
Chulalongkorn University

LIST OF TABLES

Page

Table 4.1: C_{VOL}(mGy) in each FOVs of 3D Accuitomo 170 and DLP (mGy.cm), E (μSv) in FOV 17x5, 17x12 cm^2 27
Table 4.2: DAP (mGy.cm^2) from one scan in each FOVs of Kodak 9000 3D and Kodak 9500 CB 3D and DAP (mGy.cm^2) from two and three scans in small FOV of Kodak 9000 3D..... 28
Table 5.1: Tissue weighting factors in ICRP Publication 60 versus those in ICRP Publication 103 30
Table A1: Data record form of 3D Accuitomo 170..... 35
Table A2: Data record form of Kodak 9000 3D and Kodak 9500 CB 3D 35
Table B1: kVp accuracy for the set and measured values 36
Table B2: The linearity of mAs with mGy/mAs 38
Table B3: $C_{a,100}$ of every FOVs of 3D Accuitomo 170 39
Table B4: CTDI at 90kVp, 5mA and 17.5 seconds..... 41
Table B5: Comparison of measured and system manual C_{VOL} values..... 41
Table B6: Normalized CTDI center at 90kVp, 17.5 seconds and various tube currents normalized CTDI to 5 mA 42
Table B7: CTDI peripheral at 60kVp, 5mA and 17.5 seconds..... 42
Table B8: CTDI peripheral at 70kVp, 5mA and 17.5 seconds..... 43
Table B9: CTDI peripheral at 80kVp, 5mA and 17.5 seconds..... 43
Table B10: CTDI peripheral at 90kVp, 5mA and 17.5 seconds..... 43
Table B11: Normalized CTDI peripheral at 5mA, 17.5 seconds and various kVp normalized CTDI to 90 kVp..... 43
Table C1: kVp accuracy for the set and measured values 49
Table C2: The linearity of mAs with mGy/mAs 51
Table C3: $C_{a,100}$ and tube output of Kodak 9000 3D with various kVp and mAs 52
Table C4: Comparison of measured and system manual DAP values..... 54
Table C5: Comparison of DAP from monitor with DAP value from system manual... 54

Page

Table D1: kVp accuracy for the set and measured values of medium FOV (FOV 15x9cm^2)..... 59

Table D2: kVp accuracy for the set and measured values of large FOV (FOV 20.6x18cm^2)..... 60

Table D3: The linearity of mAs with mGy/mAs of medium FOV (FOV 15x9cm^2)..... 61

Table D4: The linearity of mAs with mGy/mAs of large FOV (FOV 20.6x18cm^2)..... 62

Table D5: $C_{a,100}$ and tube output of Kodak 9500 CB 3D..... 63

Table D6: Comparison of measured and system manual DAP values..... 64

Table D7: Comparison of DAP value from monitor with DAP value from system manual..... 64

Table D8: Measured diameter distances, measured distance between Teflon pin and differences between the measured and actual distance..... 69

Table D9: Modulation Transfer Function at 10% of medium and large FOV..... 70

Table D10: Line pair per centimeter of medium and large FOV..... 71

Table D11: Mean and SD of ROI values and difference CT number..... 73

Table D12: Difference between estimated and measured CT number..... 76

จุฬาลงกรณ์มหาวิทยาลัย
Chulalongkorn University

LIST OF FIGURES

Page

Figure 1.1: Various field sizes for particular task. A shows large FOV for maxillofacial region. B shows medium FOV for maxilla/mandible. C shows small FOV for localized region..... 2
Figure 1.2: Dental arch of 6 localized regions (circles)..... 2
Figure 2.1: Cone beam CT system. X-ray source emits a cone-shaped x-ray beam directed to the area detector..... 3
Figure 2.2: Voxel dimension of CBCT system..... 6
Figure 2.3: Voxel dimension of medical CT system..... 6
Figure 3.1: Research design model..... 13
Figure 3.2: Conceptual Framework..... 14
Figure 3.3: 3D Accuitomo 170 CBCT system (left) and various FOVs (right)..... 15
Figure 3.4: Kodak 9000 3D CBCT system (left) and various FOVs; 5x3.7cm^2 (upper right), 9.3 x 5 x 3.7cm^3 (middle right), 9.3 x 7.4 x 3.7cm^3 (lower right)..... 16
Figure 3.5: Kodak 9500 cone beam 3D system (left) and 2 FOVs; 15 x 9cm^2 (upper right) and 20.6 x 18cm^2 (lower right)..... 17
Figure 3.6: Pencil ionization chamber: Unfors Xi CT detector..... 18
Figure 3.7: Unfors Xi R/F and MAM detector..... 18
Figure 3.8: Unfors Xi base unit with mAs display..... 19
Figure 3.9: Adult/Pediatric head phantom..... 19
Figure 3.10: Ionization chamber (left) and display unit (right)..... 20
Figure 3.11: CATPHAN phantom ® 600..... 20
Figure 3.12: QC kit of 3D Accuitomo 170; 3D phantom (a), wire phantom (b) and contrast phantom (c)..... 21
Figure 3.13: RANDO phantom: head and neck part..... 21
Figure 4.1: The effective dose at two FOVs (17x5 and 17x12 cm^2) of 3D Accuitomo 170..... 27
Figure 4.2: DAP of Kodak 9000 3D and Kodak 9500 cone beam 3D at various FOVs. 28

Page

Figure B1: The linearity of set and measured kVp with R^2 of 0.9995 37
Figure B2: The linearity of set kVp and tube output with R^2 of 0.9977 37
Figure B3: The linearity of mAs and mGy/mAs with R^2 of 0.8927 38
Figure B4: Tube output of various FOVs of 3D Accuitomo 170 with R^2 of 0.9419..... 39
Figure B5: Position of ionization chamber 40
Figure B6: The relation of MTF and line pairs/mm..... 44
Figure B7: Axial slice of the plain acrylic part with 5 ROIs (a) and noise, uniformity/grayscale graph (b) 45
Figure B8: Contrast scale ROI of four different materials (a) and contrast scale graph (b)..... 46
Figure B9: Mushroom image for artifact test..... 47
Figure B10: Mushroom image for patient position test 48
Figure C1: The linearity of set and measured kVp with R^2 of 0.9975 50
Figure C2: The linearity of set kVp and tube output with R^2 of 0.9955 50
Figure C3: The linearity of mAs and mGy/mAs with R^2 of 0.9014 51
Figure C4: Tube output vs kVp of Kodak 9000 3D..... 52
Figure C5: Axial view of metal rod and tubes 55
Figure C6: Measurement of distance between Teflon pins..... 56
Figure C7: Modulation transfer function VS spatial frequency graph 57
Figure D1: The linearity of set and measured kVp with R^2 0.9981 of medium FOV (FOV 15x9cm^2)..... 59
Figure D2: The linearity of set kVp and tube output with R^2 0.9984 of medium FOV (FOV 15x9cm^2)..... 59
Figure D3: The linearity of set and measured kVp with R^2 of 0.999 of large FOV (FOV 20.6x18cm^2) 60
Figure D4: The linearity of set kVp and tube output with R^2 of 0.9998 of large FOV (FOV 20.6x18cm^2)..... 60
Figure D5: The linearity of mAs and mGy/mAs with R^2 of 0.8079 of medium FOV (FOV 15x9cm^2)..... 62

Page

Figure D6: The linearity of mAs and mGy/mAs with R^2 of 0.797 of large FOV (FOV 20.6x18cm^2) 62
Figure D7: Tube output of Kodak 9500 CB 3D 63
Figure D8: Axial view of metal rod and tubes of medium FOV (a) and large FOV (b) 65
Figure D9: Axial view of circular phantom of medium FOV (a) and large FOV (b)..... 66
Figure D10: Measurement for distance accuracy between Teflon pins in medium FOV (FOV15x9cm^2) 67
Figure D11: Measurement for diameter distance accuracy in medium FOV (FOV15x9cm^2) 67
Figure D12: Measurement for distance accuracy between Teflon pins in large FOV (FOV20.6x18cm^2) 68
Figure D13: Measurement for diameter distance accuracy in large FOV (FOV20.6x18cm^2) 68
Figure D14: Modulation transfer function vs spatial frequency graph of medium FOV 70
Figure D15: Modulation transfer function vs spatial frequency graph of large FOV.... 70
Figure D16: Image of 21 line pairs per centimeter of medium FOV (a) and large FOV (b) 71
Figure D17: ROI position for measurement 72
Figure D18: Measurement of 5 ROI in different position. Central ROI used for CT number and image noise; peripheral and central ROI used for uniformity. 73
Figure D19: Axial view of phantom section CTP 486 used for inspection of artifact .. 74
Figure D20: Measurement of CT number for each material of medium FOV (a) and large FOV (b) 75
Figure D21: The linearity of CT number with R^2 of 0.9148 of medium FOV 76
Figure D22: The linearity of CT number with R^2 of 0.9046 of large FOV 76

LIST OF ABBREVIATIONS

ABBREVIATION	TERMS
°	Degree
.com	Commercial
%	Percent
∅	Diameter
Σ	Sigma, Summation symbol
μ	Attenuation coefficient
μGy	MicroGray
μSv	MicroSievert
3D	Three-dimension
a-Si	Amorphous silicon
ALARA	As low as reasonably achievable
$C_{a,100}$	CT air kerma index measured free in air integrated over 100mm
CB	Cone beam
CBCT	Cone beam computed tomography
CCD	Charge coupled device
cm	Centimeter
cm^{-1}	Per centimeter
cm^{2}	Centimeter square
cm^{3}	Cubic centimeter
CMOS	Complementary metal oxide semiconductor
$C_{PMMA,100}$	CT air kerma index measured inside PMMA integrated over 100mm
$C_{PMMA,100,c}$	CT air kerma index measured inside PMMA at center integrated over 100mm
$C_{PMMA,100,p}$	CT air kerma index measured inside PMMA at peripheral integrated over 100mm
Corp	Corporation
CT	Computed tomography
CTDI	CT dose index
CV	Coefficient of variation
C_{VOL}	Volume CT air kerma index

จุฬาลงกรณ์มหาวิทยาลัย
Chulalongkorn University

ABBREVIATION	TERMS
C_W	Weighted CT air kerma index
D	Depth
DAP	Dose area product
DLP	Dose length product
D_T	Average absorbed dose of tissue T
D_{Ti}	Average absorbed dose of tissue T in slice i
E	Effective dose
E_{DLP}	Conversion coefficient which is region-specific normalized effective dose
e.g	Exempli gratia, for example
et al	Et alibi, and others
FBP	Filtered back projection
f_i	Fraction of tissue T in slice i
FOV	Field of view
FPD	Flat panel detector
Gy	Gray
$Gy.cm^2$	Gray.centimeter square
$Gy.m^2$	Gray.meter square
H	Height
H_T	Equivalent dose of tissue T
http	Hypertext Transfer Protocol
HU	Hounsfield units
ICRP	International Commission on Radiological Protection
II	Image intensifier
Inc	Incorporation
j	each serial or helical scan
K	Air kerma
kV	Kilovoltage
kVp	Kilovoltage peak
K(z)	Air kerma along the rotation axis
l	distance of couch moving per helical rotation
lp/cm	Line pair per centimeter
lp/mm	Line pair per millimeter
mA	Milliampere

จุฬาลงกรณ์มหาวิทยาลัย
Chulalongkorn University

ABBREVIATION	TERMS
mAs	Milliampere-second
Mfg	Manufacturing
mGy	MilliGray
mGy.cm	MilliGray.centimeter
$mGy.cm^2$	MilliGray.centimeter square
mGy/mAs	Tube output in milliGray per milliampere-second
MIP	Maximum intensity projection
mm	Millimeter
mm^2	Millimeter square
MPR	Multiplanar reformation
mSv	MilliSievert
$mSv.mGy^{-1}.cm^{-1}$	MilliSievert per milliGray.centimeter
MTF	Modulation transfer function
N	Number of slices
p	Pitch
P_{KA}	Air kerma area product
$P_{KL,CT}$	CT air kerma–length product
PMMA	Polymethyl methacrylate
QC	Quality control
R^2	R-square
ROI	Region of interest
SD	Standard deviation
T	Nominal thickness
TLD	Thermoluminescent dosimeter
TMJ	Temporomandibular joint
USA	United States of America
W	Width
W_R	Radiation weighting factor
W_T	Tissue weighting factor
www	World wide web

จุฬาลงกรณ์มหาวิทยาลัย
Chulalongkorn University

CHAPTER I
INTRODUCTION

1.1. Background and Rationale

Cone beam computed tomography (CBCT) has been developed for dentistry since the late 1990s. Its advantages against medical CT are less expensive and compact size to be able to install in dental office [1]. Furthermore, limited-volume scanning is available [2] and the radiation dose is relatively low [2-4].

Even though the dose from CBCT is low, the increasing use in dentistry to assess bone dimension for dental implant placement, impacted tooth (the proximity of lower third molar to mandibular canal), osseous degenerative change of temporomandibular joint (TMJ), fracture of teeth and facial structure, bony pathology [2, 5] are major concern.

Currently, there are many available CBCT devices from different manufacturers. Each device provides variety of field of views (FOVs), making it possible to select appropriate field of view for particular task [6] such as large FOV for maxillofacial region, medium FOV for maxilla/mandible and small FOV for localized region (figure 1.1). In full dental arch, it can be divided into 6 localized regions; upper right posterior region, upper anterior region, upper left posterior region, lower left posterior region, lower anterior region and lower right posterior region (figure 1.2).

In practice, some areas are not adjacent to each other, such as upper right molar region and lower anterior region referred to undertake this technique. Thus the appropriate decision to choose one large field of view, medium field of view or multi-small field of views should be considered based on clinical applications and ALARA principle.

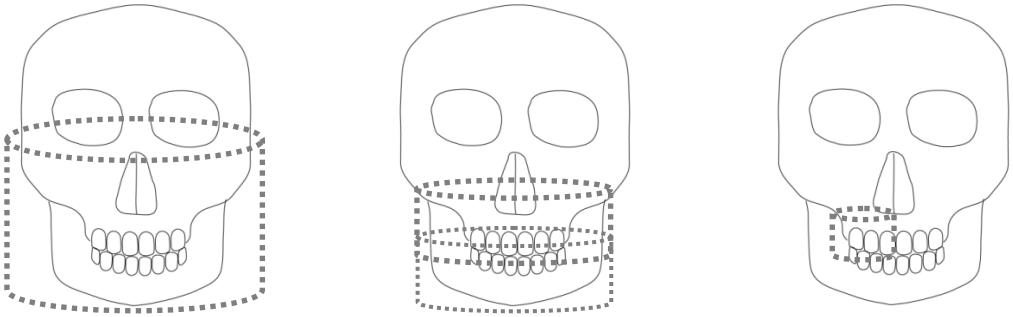

A B C

Figure 1.1: Various field sizes for particular task. A shows large FOV for maxillofacial region. B shows medium FOV for maxilla/mandible. C shows small FOV for localized region.

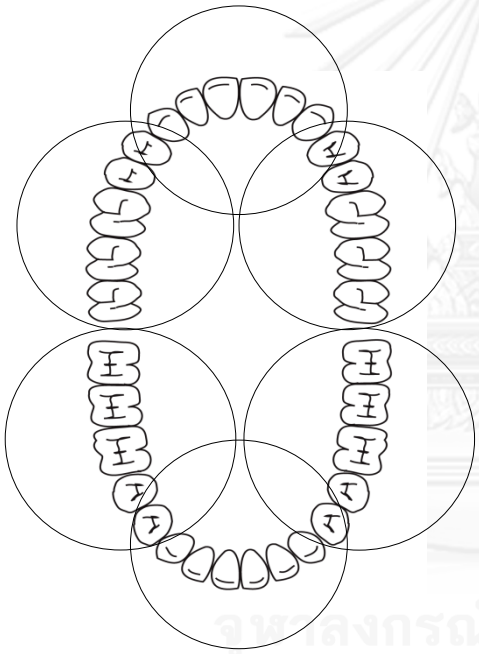

Figure 1.2: Dental arch of 6 localized regions (circles)

จุฬาลงกรณ์มหาวิทยาลัย
Chulalongkorn University

1.2. Objective

1.2.1. To study the effect of number of scans and field of views such as large, medium and multi-small, on the radiation dose in the phantom study.

CHAPTER II
REVIEW OF RELATED LITERATURE

2.1. Theory

2.1.1. Principle of Cone Beam Computed Tomography [1, 2]

Cone beam computed tomography (CBCT) is the advance technique providing images of region of interest in three orthogonal planes (axial, coronal and sagittal). The system consists of an x-ray source and the detector mounted on the opposite side of the x-ray source. The gantry will rotate around a fulcrum that fixed within the center of the region of interest. During the rotation, the x-ray source emits a cone-shaped beam of x-rays directed to the area detector (figure 2.1). The receptor detects attenuated beam by the patient. These recordings constitute the raw data that is reconstructed by a computer algorithm to generate cross-sectional images.

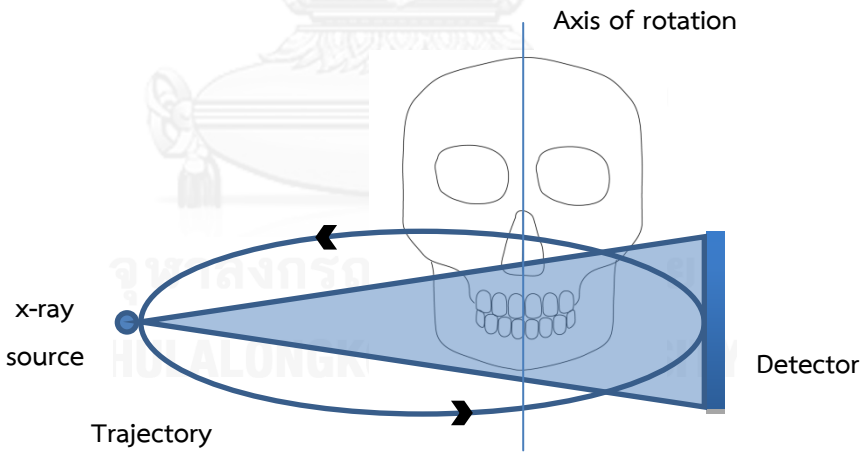

Figure 2.1: Cone beam CT system. X-ray source emits a cone-shaped x-ray beam directed to the area detector.

Because of beam geometry and a two-dimensional array used in cone beam scanner, the entire region of interest is exposed in one rotational scan and enough data is acquired for image reconstruction.

2.1.2. Image acquisition [1, 2]

Four components for image acquisition are (1) CBCT system (2) image detection system (3) image reconstruction and (4) image display.

2.1.2.1. CBCT system: Image acquisition

There are three possible patient positions in CBCT system: (1) sitting (2) standing and (3) supine. Immobilization of the patient's head during the rotation scan is required for all systems because the patient movement degrades the image quality.

Two types of exposure in CBCT system are continuous radiation exposure and pulse radiation exposure which the actual exposure time is markedly less than the scanning time. In acquiring an image, the detector samples the attenuated beam in its trajectory. For continuous x-ray beam, some of which does not contribute to the formation of the image. In contrast, pulse x-ray beam coincides with the detector sampling. Thus the latter reduces the patient radiation dose considerably.

The shape of the scan volume can be either cylindrical or spherical shape. It depends on the detector size and shape, the beam projection geometry and the ability to collimate the beam. Collimation of the primary x-ray beam limits x-ray exposure to the region of interest. Currently, various FOVs are available. They vary from few centimeters in diameter and height to a full head size. FOVs can be divided into 5 categories according to scan volume height as the followings:

Localized region: approximately 5 cm or less (e.g., dentoalveolar region)

Single arch: 5 to 7 cm (e.g., maxilla or mandible)

Interarch: 7 to 10 cm (e.g., both mandible and maxilla)

Maxillofacial region: 10 to 15 cm (e.g., mandible extending to Nasion)

Craniofacial region: greater than 15 cm (e.g., from lower border of mandible to the vertex of head)

Chulalongkorn University

Moreover, the FOV can be divided into 3 categories according to the region of interest as the followings [7]:

Large FOV: for maxillofacial/craniofacial region

Medium FOV: for maxilla/mandible

Small FOV: for localized region

A partial or full rotational scan can be performed while x-ray source and a reciprocating area detector move synchronously around a fixed fulcrum within the patient head. During the rotation, each projection image is made by sequential single-image capture of attenuated x-ray beams by the detector. The complete series of the projection images refer to the projection data.

Frame rate is measured in frames or projection images per second. The maximum frame rate and the rotational speed determined the number of projection acquired. With higher frame rate, more information is received to reconstruct the image, thus the signal to noise ratio increases. However, more projection data result in longer scan time, higher patient dose and longer primary reconstruction time. Reducing scan time is desirable in order to reduce motion artifact resulting from subject movement. This can be achieved by reduce number of projection or reduce the scan arc. When the patient dose is reduced, the images are produced by this method with greater noise.

2.1.2.2. Image detection system [2, 8]

จุฬาลงกรณ์มหาวิทยาลัย
Chulalongkorn University

The detectors of CBCT system are image intensifiers/charge-coupled device (II/CCD) combination, complementary metal oxide semiconductor (CMOS) and amorphous silicon flat panel detectors (a-Si FPD). Image intensifier may create geometric distortion which reduces the measurement accuracy, whereas flat panel detectors do not suffer this problem. However, flat panel detector has limitation in its own performance that related to non-uniformity response and dead-nonfunctional pixel. These problems can be overcome by system calibration and correction algorithm. Comparison to FPD, CMOS has smaller pixel size which provides higher resolution. However, unlike FPD, it's difficult to produce a single CMOS chip in a large size. To overcome this problem, the common technique is tiling multiple CMOS chips to form a larger mosaic.

A reduction in pixel size is desirable because of higher spatial resolution. However, smaller pixel size captures fewer x-ray photons results in more image noise. Thus greater radiation is required and the patient dose is higher.

In CBCT system, the voxel dimension depends on the pixel size on the area detector. Therefore, in general, CBCT system provides voxel resolution that is isotropic or equal in all three dimensions (figure 2.2). Contrast to medical CT system of which voxel dimension depends on slice thickness, the voxel is anisotropic or columnar with height being different from the width and depth dimension (figure 2.3).

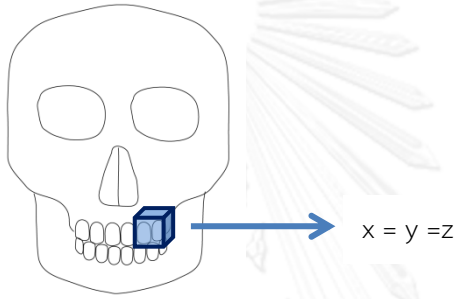

Figure 2.2: Voxel dimension of CBCT system

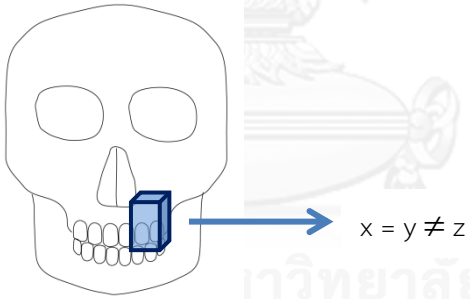

Figure 2.3: Voxel dimension of medical CT system

2.1.2.3. Image reconstruction [1, 2]

Once the projection data is acquired, the data must be processed to generate the volumetric data set by applying the software program incorporating sophisticated algorithms including filtered back projection (FBP). This process is the primary reconstruction.

Reconstruction time varies, depending on the acquisition parameters (voxel size, FOV, number of projections), hardware (processing speed, data throughput from acquisition to

workstation computer) and software (reconstruction algorithms). Reconstruction should be completed in an acceptable time, less than 3 minute for standard scans, to compliment the patient flow.

2.1.2.4. Image display [1, 2]

Volumetric data is presented on the screen to the clinician as secondary images in three orthogonal planes. Optimal visualization of images depends on the adjustment of window width and window level to bone and the application of specific filters.

Images can be presented in non-orthogonality by using software referred to as multiplanar reformation (MPR) such as oblique mode, curved planar reformation and serial transplanar reformation. Furthermore, any multiplanar image can be presented in thickened image by increasing the number of adjacent voxels included in the display. This is referred to as ray sum. Full thickness perpendicular ray sum image can be used to create simulated projection such as lateral cephalometric image. Unlike conventional radiograph, this ray sum image is without magnification and parallax distortion.

Three-dimensional image (3D image) can be generated by using volume rendering techniques of which two specific techniques are available. One is indirect volume rendering. This is a complex process requiring selection of the intensity or density of the grayscale level in voxels within an entire data set (segmentation) to be displayed. The other is direct volume rendering which is much simpler process. The most common technique is maximum intensity projection (MIP) which evaluated each voxel value along an imaginary projection from an observer's eyes within a volume of interest and then presenting only the highest value as the display value.

Chulalongkorn University

2.1.3. Quantities for CT dosimetry

2.1.3.1. CT air kerma index [9]

The CT air kerma index, $C_{a,100}$, measured free in air for a single rotation of a CT scanner is the integral of the air kerma along a line parallel to the axis of rotation of the scanner over a

length of 100 mm divided by the nominal thickness, T. The integration range is positioned symmetrically about the volume scanned, thus:

$$C_{a,100} = \frac{1}{T}\int_{-50}^{+50} K(z)dz$$

where K(z) is air kerma (Gy) along the rotation axis and T is nominal thickness (mm).

For a multislice scanner with N simultaneously acquired slices of nominal thickness T (nominal width of irradiated beam NT), $C_{a,100}$ becomes:

$$C_{a,100} = \frac{1}{NT}\int_{-50}^{+50} K(z)dz$$

where N is number of slices.

The CT air kerma index measured inside PMMA head and body phantoms, is defined similarly to $C_{a,100}$ and can be written in $C_{PMMA,100}$.

The weighted CT air kerma index, C_W, combines values of $C_{PMMA,100}$ measured at the center and periphery of a standard CT dosimetry phantom. It is given by:

$$C_W = \frac{1}{3}(C_{PMMA,100,c} + 2C_{PMMA,100,p})$$

A further quantity, C_{VOL}, takes into account the helical pitch or axial scan spacing, thus:

$$C_{VOL} = C_W \frac{NT}{l} = \frac{C_W}{p}$$

where l is distance of couch moving per helical rotation and p is pitch defines as total distance of couch moving divided by number of slices and nominal thickness.

Note: In CBCT, tube moves around the patient in single rotation without couch/chair moving and beam is emitted in cone-shaped. Thus the pitch is equal to 1.

The CT air kerma–length product determined for the standard CT dosimetry phantom and a complete CT examination, $P_{KL,CT}$, is calculated using

$$P_{KL,CT} = \sum_j C_{VOL} l$$

where j is each serial or helical scan and l is scan length.

Note: In CBCT, scan length is equal to height of FOV.

2.1.3.2. Effective dose [9-12]

The effective dose is a quantity used as indicator of overall patient dose that related to detriment arising from stochastic effects. It was defined by International Commission on Radiological Protection (ICRP) Publication 60 (1991) as the sum of product of equivalent dose (consider the radiation type) to the organ or tissue and a tissue weighting factor, W_T, for that organ of tissue (ICRP Publication 103).

To allow comparison with other types of examination, there is sometimes a need to assess the effective dose. Estimation of effective dose for CT procedures can be obtained from the product of DLP value and conversion coefficient as the following formula:

$$E = DLP\ x\ E_{DLP}$$

where E is effective dose and E_{DLP} is conversion coefficient which is region-specific normalized effective dose ($mSv.mGy^{-1}.cm^{-1}$) such as E_{DLP} in head region equals to 0.0023 $mSv.mGy^{-1}.cm^{-1}$.

2.1.3.3. Air kerma area product [9]

The air kerma area product, P_{KA}, is the integral of the air kerma (K) over the area of the x-ray beam in a plane perpendicular to the beam axis. Thus

$$P_{KA} = \int_A K(x,y)dxdy$$

The unit of air kerma area product is $Gy.m^2$ or $Gy.cm^2$.

The useful property of air kerma area product is that it is approximately invariant with the distance from x-ray source. Thus the measurement plane does not need to be close to the patient or phantom that there is a significant contribution from backscattered radiation.

2.2. Review of Related Literature

Ludlow JB et al [3] compared dosimetry of 3 CBCT devices: CB Mercuray (FOVs: 30.48cm (12inches), 22.86cm (9inches), 15.24cm (6inches)), NewTom 3G (FOV: 30.48cm (12inches)) and i-CAT (FOVs: 30.48cm (12inches), 22.86cm (9inches)). Dose measurement was performed by placing

thermoluminescent dosimeters (TLDs) in 24 sites throughout the layer of head and neck of RANDO phantom. Exposure parameters (kVp, mAs) of CB Mercuray; NewTom 3G and i-CAT were 100, 100; 110, 8.1 and 120, 37.3 respectively. Three exposures were made without changing the position of the phantom for each CBCT examination. Doses from TLDs at different positions within a tissue or organ were averaged. These doses and percent of tissue irradiated were used to calculate radiation equivalent dose (H_T). Effective dose (E) could be calculated by using H_T and tissue weighting factor from ICRP 1990 and proposed 2005. For CB Mercuray FOV 30.48cm; 22.86cm; 15.24cm, $E_{(ICRP1990\ and\ ICRP2005draft)}$ were 476.6, 557.6; 288.9, 435.5; 168.4, 283.3μSv respectively. For NewTom 3G FOV 30.48cm, $E_{(ICRP1990\ and\ ICRP2005\ draft)}$ was 44.5, 58.9μSv. For i-CAT FOV 30.48cm; 22.86cm, $E_{(ICRP1990\ and\ ICRP2005draft)}$ were 134.8, 193.4; 68.7, 104.5μSv respectively. In this study, it was found that CBCT dose depended on the devices and FOVs.

Hirsch E et al [6] compared absorbed doses and effective doses of 2 CBCT devices: Veraviewepocs 3D (FOV: 4x4, 4x4+panoramic and 8x4cm^2) and 3D Accuitomo (FOV: 4x4 and 6x6cm^2). Dose measurement was performed by placing TLDs in 16 sites in head and neck of anthropomorphic phantom. Anterior region of maxilla was scanned three times for each technique in order to ensure reliability. Doses from TLDs that located in the same tissue or organ were averaged. These doses calculated into equivalent dose by the formula: $H_T = \sum W_R \times D_T$ where H_T is equivalent dose, W_R is radiation weighting factor, D_T is average absorbed dose. The effective dose (E) is calculated by the formula: $E = \sum W_T \times H_T$ where W_T is tissue weighting factor proposed by ICRP 2005. E for 3D Accuitomo 4x4cm^2 was 20.02μSv and for 6x6cm^2 was 43.27 μSv. E for Veraviewepocs 3D 4x4cm^2 was 30.24μSv, for 4x4cm^2+panoramic was 29.78μSv and for 8x4cm^2 was 39.92μSv. The smaller FOV provided less doses than larger FOV. However the radiation dose from 4x4cm^2+panoramic was lower than dose from 4x4cm^2 because panoramic probably leads to lower dose than two scouts.

Lofthag-Hansen S et al [13] measured the dose area product (DAP) of 2 CBCT devices (3D Accuitomo and 3D Accuitomo FPD) with different exposure parameters (60-80 kVp, 1-10 mA). Field size for 3D Accuitomo was 30x40mm^2 and for 3D Accuitomo FPD were 40x40 and 60x60mm^2. DAP values were measured using a plane-parallel transmission ionization chamber connected to electrometer. At 80 kVp, DAP value increased with higher mA. With the same tube current, DAP was three times higher for 60x60mm^2 FOV than 30x40mm^2 FOV. For each tube current (2, 4, 6, 8 or 10mA), a change of 10kVp increased DAP 30-40%. From this result, it was found that radiation dose varied with the field size, kVp and mA. The DAP value increased with higher mA, kVp and larger field size.

Pauwels R et al [7] estimated the absorbed organ dose and effective dose of 14 CBCT devices from 10 manufacturers with different exposure parameters (70-120 kVp, 8.8-169 mAs). Two similar types of anthropomorphic male Alderson Radiation Therapy phantoms were used. 147 TLDs were placed throughout head and neck for one phantom and 152 TLDs for the other. Equivalent dose was calculated from the formula: $H_T = W_R \sum f_i D_{Ti}$ where H_T is equivalent dose, W_R is radiation weighting factor (being 1 for x-ray), f_i is the fraction of tissue T in slice i and D_{Ti} is average absorbed dose of tissue T in slice i. Effective dose (E_T) was calculated from the formula: $E_T = W_T \times H_T$ where W_T is tissue weighting factor recommended by ICRP103. Due to large difference in acquired volume, the results were split up by dividing field size into three categories: large FOV (for maxillofacial region), medium FOV (for dentoalveolar region) and small FOV (for localized region). The average effective doses for large FOV, medium FOV and small FOV were 131, 88 and 34μSv respectively. The result indicated that the dose depends on the field size.

From literature review, the radiation dose from various FOVs had been studied and presented in dose from one scan, so it is quite interesting to study the radiation dose from different number of scans of various FOVs.

จุฬาลงกรณ์มหาวิทยาลัย
Chulalongkorn University

CHAPTER III

RESEARCH METHODOLOGY

3.1. Research Design

This study is an experimental study (in vitro).

3.2. Keywords

- Cone beam computed tomography
- CBCT
- Dosimetry
- Multi-small field of views
- DAP

จุฬาลงกรณ์มหาวิทยาลัย
Chulalongkorn University

3.3. Research Design Model

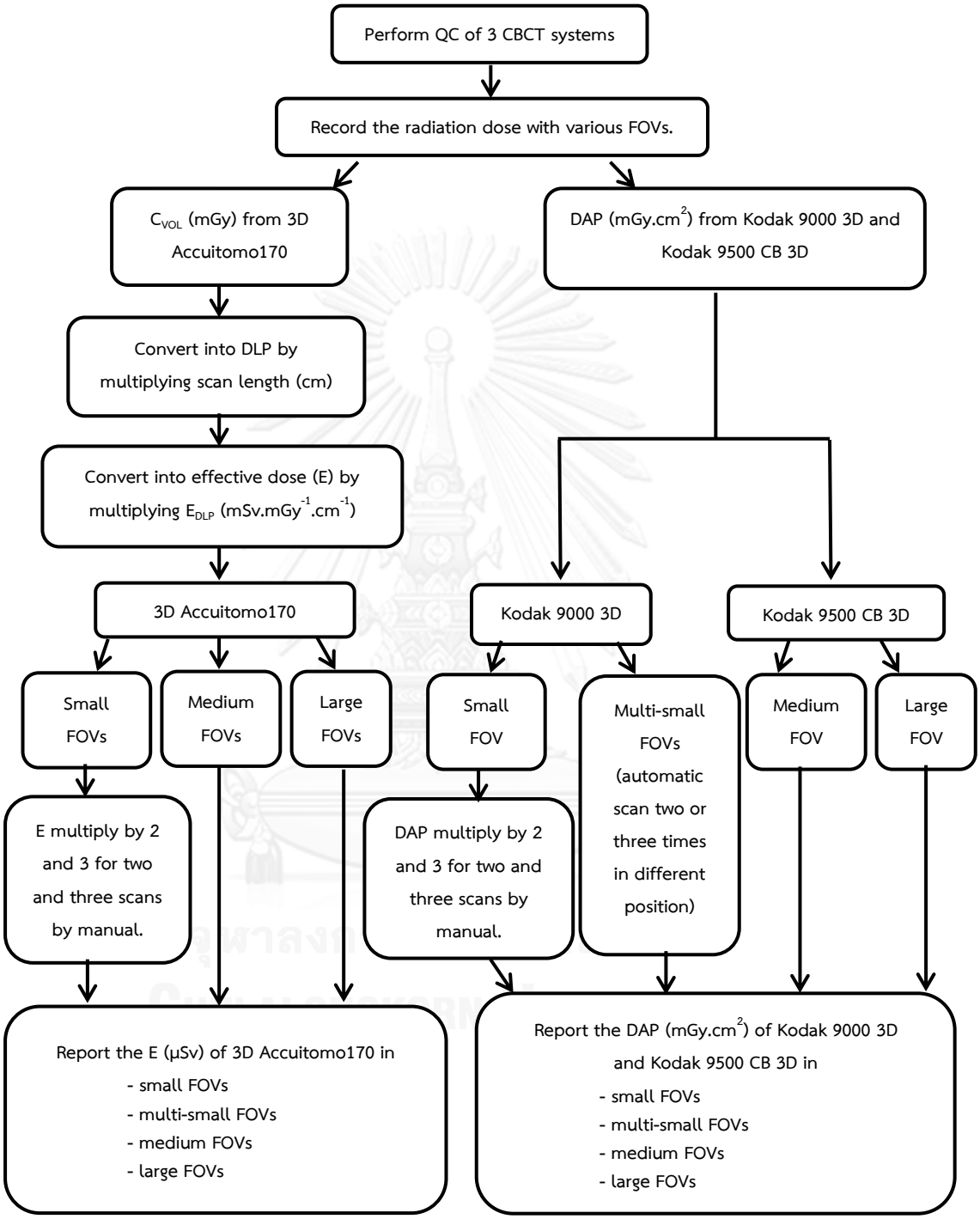

Figure 3.1: Research design model

3.4. Conceptual Framework

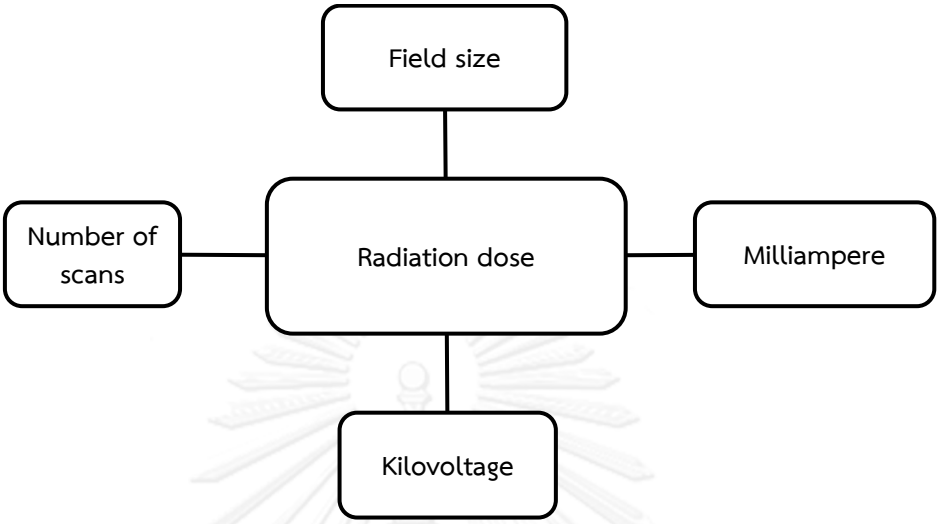

Figure 3.2: Conceptual Framework

In this study, the variable factors are field size and number of scans.

3.5. Research Question

What is the radiation dose when using different number of scans of various FOVs?

จุฬาลงกรณ์มหาวิทยาลัย
Chulalongkorn University

3.6. Material

3.6.1. CBCT devices

Three CBCT devices will be used in this study.

3.6.1.1. 3D Accuitomo 170 (J. MORITA Mfg. Corp., Kyoto, Japan) [14]

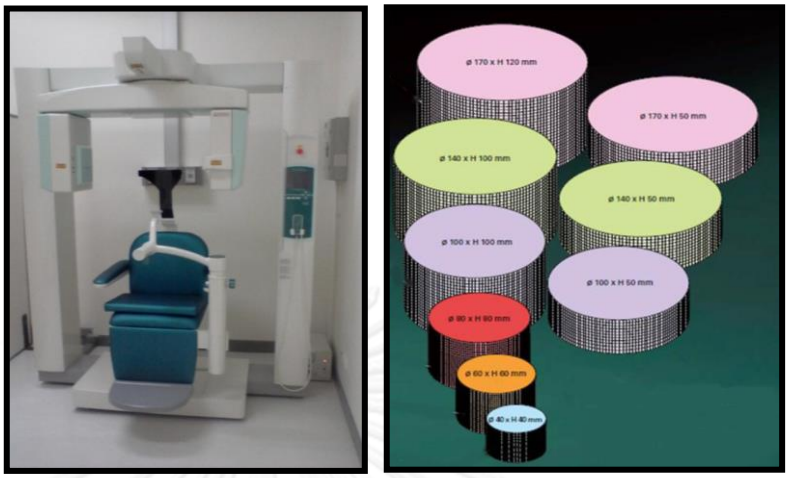

Figure 3.3: 3D Accuitomo 170 CBCT system (left) and various FOVs (right) [14]

Trade name:	3D Accuitomo XYZ Slice View Tomograph
Model:	MCT-1
Tube voltage:	60-90 kV
Tube current:	1-10 mA
Exposure time:	17.5 seconds (for standard mode: full scan 360°)
Tube focal spot	0.5 mm
Type of exposure	Continuous radiation exposure
Field size:	9 field of views (FOVs) in diameter(cm) x height (cm): 4x4, 6x6, 8x8, 10x5, 10x10, 14x5, 14x10, 17x5 and 17x12.
SID:	842 mm (4x4, 6x6, 8x8, 10x5, 10x10, 14x5 and 14x10), 744 mm (17x5 and 17x12)
SOD:	540 mm
Detector:	Amorphous silicon flat panel detector (a-Si FPD)
Software:	i-Dixel software

จุฬาลงกรณ์มหาวิทยาลัย
Chulalongkorn University

3.6.1.2. Kodak 9000 3D Extraoral Imaging System (Carestream health, Inc., New York, USA) [15]

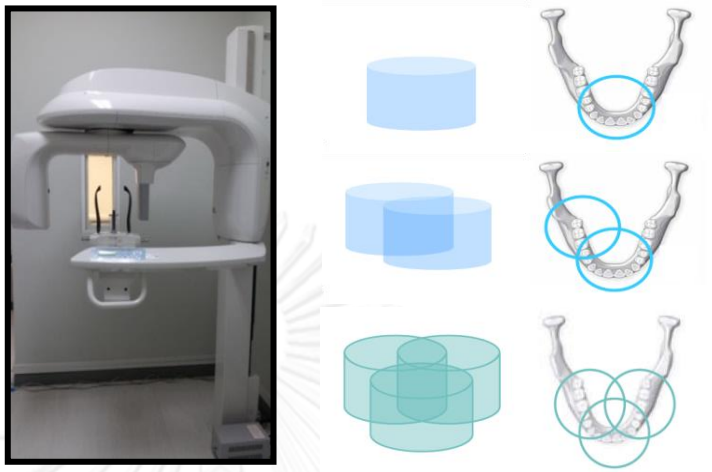

Figure 3.4: Kodak 9000 3D CBCT system (left) and various FOVs; 5x3.7cm^2 (upper right), 9.3 x 5 x 3.7cm^3 (middle right), 9.3 x 7.4 x 3.7cm^3 (lower right). [15]

Model:	KODAK 9000 3D
Tube voltage:	60-90 kV
Tube current:	2-15 mA (2, 2.5, 3.2, 4, 5, 6.3, 8, 10, 12, 15 mA)
Exposure time:	10.8 seconds
Tube focal spot	0.5 mm
Type of exposure	Pulse radiation exposure
Field size:	3 FOVs, one is single volume in diameter (cm) x height (cm): 5 x 3.7 (single volume) and the other two are multi-volume (stitching) in WxDxH (cm^3): 9.3 x 5 x 3.7 (2 volumes) and 9.3 x 7.4 x 3.7 (3 volumes).
SID:	690 mm
SOD:	440 mm
Detector:	CMOS Sensor with Optical Fiber
Software:	Kodak Dental Imaging Software and CS 3D imaging software

จุฬาลงกรณ์มหาวิทยาลัย
Chulalongkorn University

3.6.1.3. Kodak 9500 Cone Beam 3D System (Carestream health, Inc., New York, USA) [16]

Figure 3.5: Kodak 9500 cone beam 3D system (left) and 2 FOVs; 15 x 9cm^2 (upper right) and 20.6 x 18cm^2 (lower right). [16]

Model:	K9500 3D
Tube voltage:	60-90 kV
Tube current:	2-15 mA (2, 2.5, 3.2, 4, 5, 6.3, 8, 10, 12, 15 mA)
Exposure time:	10.8 seconds
Tube focal spot	0.7 mm
Type of exposure	Pulse radiation exposure
Field size:	2 field of views (FOVs) in diameter (cm) x height (cm): 15x9 and 20.6x18.
SID:	770 mm
SOD:	540 mm
Detector:	Amorphous silicon flat panel detector (a-Si FPD)
Software:	Kodak Dental Imaging Software and OnDemand3D application

จุฬาลงกรณ์มหาวิทยาลัย
CHULALONGKORN UNIVERSITY

3.6.2. QC material

3.6.2.1. Unfors Raysafe Xi dosimeter

3.6.2.1.1. Pencil ionization chamber: Unfors Xi CT detector

CT dose will be measured in dose (mGy or µGy) and automatic correction of temperature and pressure will be applied for all dose measurement.

Figure 3.6: Pencil ionization chamber: Unfors Xi CT detector

3.6.2.1.2. Unfors Xi R/F and MAM detector

The R/F detector measures kVp, dose, dose rate, pulse, pulse rate, dose/frame, time, HVL and waveforms simultaneously.

Figure 3.7: Unfors Xi R/F and MAM detector

3.6.2.1.3. Unfors Xi base unit with mAs display

The results of measured parameters are shown on three row alphanumerical display. It's compatible and interchangeable with all Unfors Xi detectors.

Figure 3.8: Unfors Xi base unit with mAs display

3.6.2.2. PMMA 16 cm diameter cylindrical phantom

Manufacturer: FLUKE Biomedical

Model: 76-419-4150 (CT Dose Phantom Kit for Adult/Pediatric Head and body)

In this study, Adult/Pediatric head phantom will be used.

จุฬาลงกรณ์มหาวิทยาลัย
Chulalongkorn University

Figure 3.9: Adult/Pediatric head phantom

3.6.2.3. DAP meter: PTW Freiburg Model Diamentor E

Figure 3.10: Ionization chamber (left) and display unit (right)

3.6.2.4. CATPHAN phantom® 600

Figure 3.11: CATPHAN phantom® 600

3.6.2.5. QC kit of 3D Accuitomo 170

There are 3 phantoms of QC kit of 3D Accuitomo 170. All phantoms have diameter and height of 5 cm. First is 3D phantom with mushroom-shaped at center. Second is wire phantom that consists of PMMA tube with vertical 0.1mm stainless steel wire. Third is contrast phantom that consists of PMMA cylinder with air, PMMA, bone equivalent plastic and aluminum blocks at center axis.

จุฬาลงกรณ์มหาวิทยาลัย
Chulalongkorn University

a b c

Figure 3.12: QC kit of 3D Accuitomo 170; 3D phantom (a),
wire phantom (b) and contrast phantom (c)

3.6.3. RANDO phantom: head and neck part

Figure 3.13: RANDO phantom: head and neck part

In this study, RANDO phantom was used to simulate the patient in positioning.

จุฬาลงกรณ์มหาวิทยาลัย
Chulalongkorn University

3.7. Methods

3.7.1. Perform QC of 3 CBCT devices according to manufacturer's guideline in order to verify the radiation dose from manual.

3.7.1.1. Dose measurement

3.7.1.1.1. CTDI measurement in 3D Accuitomo 170

3.7.1.1.2. DAP measurement in Kodak devices

(Dose measurement will be performed three times.)

3.7.1.2. Image quality

3.7.1.2.1. 3D Accuitomo 170: spatial resolution test, noise, uniformity / grayscale and contrast resolution test, artifact test, patient position test

3.7.1.2.2. Kodak 9000 3D: rotative arm axis, spatial linearity, MTF measurement

3.7.1.2.3. Kodak9500 CB 3D: rotative arm axis, circular symmetry and spatial linearity, MTF measurement, high resolution measurement, CT number accuracy, noise, uniformity and image artifact, CT number linearity

จุฬาลงกรณ์มหาวิทยาลัย
CHULALONGKORN UNIVERSITY

3.7.2. Record the radiation doses using RANDO phantom for each scan of large, medium and small FOVs of 3 CBCT devices. Acquisition parameters are 80kVp, 5mA and 17.5 seconds (for 3D Accuitomo 170), 10.8 seconds (for Kodak systems).

3.7.2.1. In 3D Accuitomo170, dose will be recorded in C_{VOL} (mGy) and convert into DLP by the following formula:

$$DLP = C_{VOL} X\, l \qquad (1)$$

where DLP is dose length product (mGy.cm),
C_{VOL} measured in mGy,
l is scan length (cm).

DLP will be converted into effective dose (E) by the following formula:

$$E = DLP\ X\ E_{DLP} \qquad (2)$$

where E(effective dose): mSv
DLP: mGy.cm
E_{DLP} (conversion coefficient): 0.0023 mSv.mGy^{-1}.cm^{-1} [10]

3.7.2.2. In Kodak 9000 3D and Kodak 9500 CB 3D, dose will be recorded in DAP (mGy.cm^2).

3.7.3. Divide FOVs into 3 categories

3.7.3.1. Small FOVs (diameter, cm x height, cm): 4x4, 6x6, 5x3.7 and multi-small FOVs (W x D x H (cm^3)): 9.3x5x3.7, 9.3x7.4x3.7

3.7.3.2. Medium FOVs (diameter, cm x height, cm):8x8, 10x5, 10x10, 14x5, 14x10, 17x5, 15x9

3.7.3.3. Large FOVs (diameter, cm x height, cm): 17x12, 20.6x18

3.7.4. In order to get larger field size in small FOV, two or three scans were performed. Doses, E and DAP, are obtained by multiplying both parameters of a single exposure by 2 or 3.

จุฬาลงกรณ์มหาวิทยาลัย
Chulalongkorn University

3.7.5. Report the E of 3D Accuitomo170 and DAP of Kodak 9000 3D and Kodak 9500 CB 3D in small, multi-small, medium and large FOVs.

3.8. Data Analysis

Radiation dose of one, two and three scans of small FOV and one scan of medium-large FOV will be reported.

3.9. Sample Size Determination

Total number of sample size was calculated from summation of variable field of views. Those are: 9 FOVs for 3D Accuitomo170, 3 FOVs for Kodak 9000 3D, 2 FOVs for Kodak 9500 CB 3D. Therefore, the total numbers of sample size are 9+3+2 or 14 scans.

3.10. Statistical Analysis

Mean of air kerma (mGy) and DAP ($mGy.cm^2$).

จุฬาลงกรณ์มหาวิทยาลัย
Chulalongkorn University

3.11. Outcome Measurement

Radiation dose

- C_{VOL} : mGy
- E : μSv
- DAP : $mGy.cm^2$

3.12. Expected Benefit

An appropriate field of view and number of scans to reduce radiation dose can be implemented to the clinical studies.

3.13. Ethical Considerations

Although this study is performed in phantom, the research proposal will be submitted for approval by Ethics Committee of Faculty of Medicine, Chulalongkorn University and Faculty of Dentistry, Mahidol University.

Note: The research proposal has been approved by Ethics Committee of Faculty of Medicine, Chulalongkorn University and Faculty of Dentistry, Mahidol University.

จุฬาลงกรณ์มหาวิทยาลัย
Chulalongkorn University

CHAPTER IV
RESULTS

4.1. Quality control of the CBCT systems

The results of quality control of three CBCT systems (3D Accuitomo 170, Kodak 9000 3D and Kodak 9500 Cone Beam 3D) are shown in Appendix B-D.

4.2. Dose measurement

The results of dose measurement are shown in table 4.1-4.2 and figure 4.1-4.2.

จุฬาลงกรณ์มหาวิทยาลัย
Chulalongkorn University

4.2.1. Radiation doses (C_{VOL}, DLP, E) of 3D Accuitomo 170

Table 4.1: C_{VOL}(mGy) in each FOVs of 3D Accuitomo 170 and DLP (mGy.cm), E (μSv) in FOV 17x5, 17x12 cm^2

Type of FOVs	FOVs (diameter (cm) x height (cm))	C_{VOL} (mGy)	DLP (mGy.cm)	E (μSv)
Small FOV	4x4	3.4	-	-
	6x6	4.3	-	-
Medium FOV	8x8	4.9	-	-
	10x5	6.0	-	-
	10x10	5.1	-	-
	14x5	7.3	-	-
	14x10	6.0	-	-
	17x5	7.7	38.5	88.55
Large FOV	17x12	6.4	76.8	176.64

Remark: The dose calculation for FOV 4x4, 6x6, 8x8, 10x5, 10x10, 14x5 and 14x10cm^2 are not acceptable to display in Table 4.1 for DLP and E.

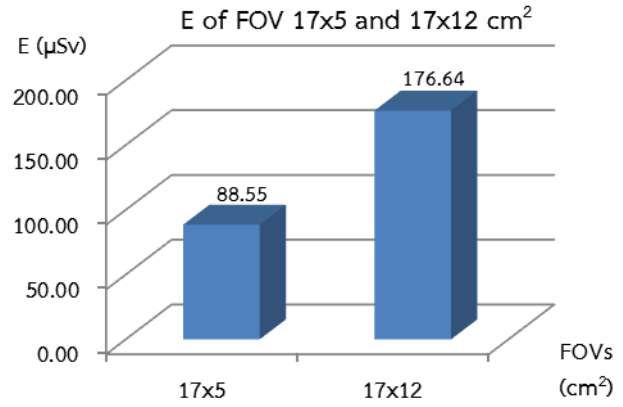

Figure 4.1: The effective dose at two FOVs (17x5 and 17x12 cm^2) of 3D Accuitomo 170

4.2.2. Radiation dose, DAP, of Kodak9000 3D and Kodak9500 Cone Beam 3D

Table 4.2: DAP ($mGy.cm^2$) from one scan in each FOVs of Kodak 9000 3D and Kodak 9500 CB 3D and DAP ($mGy.cm^2$) from two and three scans in small FOV of Kodak 9000 3D

Type of FOVs	FOVs	DAP ($mGy.cm^2$)	DAPx2 ($mGy.cm^2$)	DAPx3 ($mGy.cm^2$)
Small FOV	5x3.7	131	262	393
Multi-small FOV	9.3x5x3.7	261	-	-
	9.3x7.4x3.7	392	-	-
Medium FOV	15x9	211	-	-
Large FOV	20.6x18	502	-	-

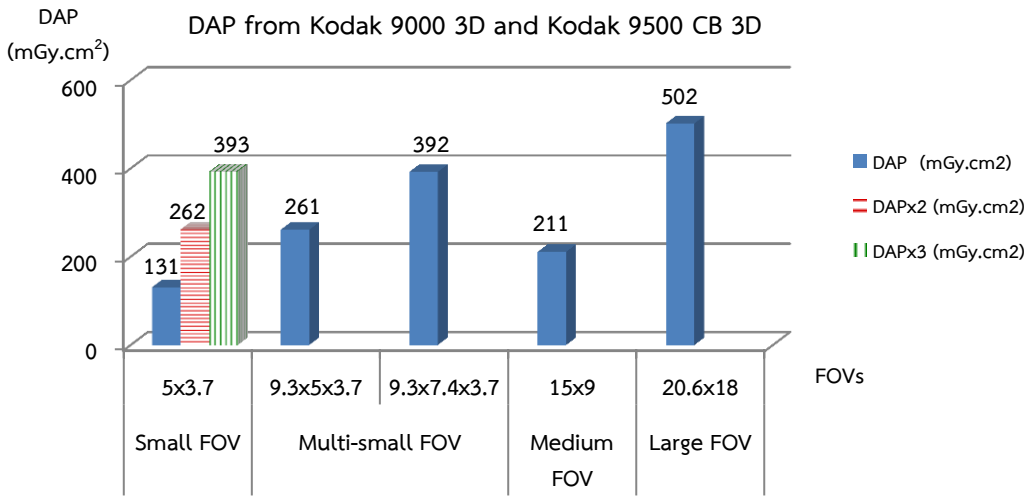

Chulalongkorn University

Figure 4.2: DAP of Kodak 9000 3D and Kodak 9500 cone beam 3D at various FOVs.

CHAPTER V
DISCUSSION AND CONCLUSION

5.1. Discussion

When a uniform phantom was positioned at the center of field of view, the dose distribution in x-y plane of full rotation scan should be symmetry with the highest dose at the center of rotation and gradient towards the peripheral, furthermore the dose distribution should drop outside the primary beam. When the phantom was positioned off-center, the dose distribution in x-y plane of full rotation scan was asymmetry with highest dose in the region of interest [13, 17, 18]. According to asymmetrical dose distribution in off-center position, CTDI would be unreliable for the effective dose estimation of small FOV, but could be reliable for large FOV with a center of rotation set in the mid-sagittal plane [13]. From our study at both small and medium FOVs, the phantom may be positioned off-center because the proper center of rotation was not identified by the manufacturer. In practice, the position of small FOV was within region of interest along the dental arch while the medium FOV, the center of rotation was located anteriorly from center to cover the jaws. Therefore, FOV 17x5 and 17x12cm^2 in 3D Accuitomo 170 were most reliable for the dose calculation of DLP and E.

Since ICRP Publication 103 (2007) has recommended the new tissue weighting factors to determine the effective dose and replace the factor recommended in ICRP Publication 60 (1991). The differences in tissue weighting factors for head and neck region are salivary glands, thyroid and remainder organs such as, lymphatic nodes and oral mucosa (Table 5.1). However, the conversion coefficient of DLP to E (E_{DLP}) based on ICRP Publication 103 is not available.

The other limitation of this study is the conversion coefficient of DAP to E for CBCT imaging. Therefore, the DAP values were reported in this study of different systems regardless of beam geometry and field sizes to simulate real condition.

จุฬาลงกรณ์มหาวิทยาลัย
Chulalongkorn University

Table 5.1: Tissue weighting factors in ICRP Publication 60 versus those in ICRP Publication 103 [12]

Tissue or organ	Tissue weighting factors in ICRP Publication 60	Tissue weighting factors in ICRP Publication 103
Gonads	0.20	0.08
Red bone marrow	0.12	0.12
Colon	0.12	0.12
Lung	0.12	0.12
Stomach	0.12	0.12
Bladder	0.05	0.04
Liver	0.05	0.04
Esophagus	0.05	0.04
Thyroid	0.05	0.04
Breast	0.05	0.12
Bone surface	0.01	0.01
Skin	0.01	0.01
Brain	Remainder organ	0.01
Salivary glands	None	0.01
Remainder organs	0.05	0.12

Note: Tissue weighting factors of lymphatic nodes and oral mucosa in remainder organs are not defined in ICRP Publication 60, but they are defined in ICRP Publication 103.

In this study, the radiation dose was determined according to field size and number of scans. In one scan, the effective dose from 3D Accuitomo 170 and DAP values from Kodak devices increased linearly with field size. Similarly, DAP values from different acquisition in Kodak9000 3D increased with number of scans. DAP values of two and three scans of small FOV (5x3.7cm^2) were 262 and 393 mGy.cm^2 respectively, which were higher than DAP value of one scan of medium FOV (211 mGy.cm^2) and the large FOV resulted in the highest value of 502 mGy.cm^2. It is highly recommended to use the medium FOV rather than two or three scans of small FOV. If the medium FOV is not available, two or three scans of small FOV are dose saving in comparison to one scan of large FOV. Similarly, Lukat TD et al [19] showed two small FOV acquisitions of bilateral TMJ provided significant less radiation dose than one scan of large FOV and recommended to take individual right and left TMJ with small FOVs (one for each TMJ) as dose reducing alternative to large FOV. However their study did not include medium FOV.

Endo A et al [20] showed DAP values of Kodak 9000 3D ranged from 260.3-296.4 mGy.cm^2. These values were higher approximately twice than this study because of the higher acquisition parameters at 70-74 kVp, 10 mA.

The UK's Health Protection Agency [21] proposed an achievable dose of 250mGy.cm^2 for CBCT imaging taken for upper first molar implant in adult procedure. In this study, DAP values of one scan of small FOV and medium FOV were less than this value, except for one scan of large FOV. It was approximately higher than twice of achievable dose. Moreover, due to large field size, critical organs such as eyes, thyroid gland, salivary glands were involved in primary beam during the scan. Thus large FOV should be chosen only when maxillofacial region is required.

The benefit of this study is the appropriate selection of FOV and number of scans according to ALARA principle.

5.2. Conclusion

The CBCT radiation dose was affected by the field size and number of scans. The radiation dose is higher when the FOVs and number of scans increase. Selection of proper FOV and number of scans result in the patient radiation dose reduction.

จุฬาลงกรณ์มหาวิทยาลัย
Chulalongkorn University

REFERENCES

[1] Scarfe, W. C. and Farman, A. G. Cone-beam computed tomography. In White, S. C. and Pharoah, M. J. (eds.), Oral Radiology Principles and Interpretation, pp. 225-35. 6th ed. St. Louis: Mosby, 2009.

[2] Scarfe, W. C. and Farman, A. G. What is cone-beam CT and how does it work? Dent Clin North Am 52 (2008): 707-30.

[3] Ludlow, J. B., Davies-Ludlow, L. E., Brooks, S. L. and Howerton, W. B. Dosimetry of 3 CBCT devices for oral and maxillofacial radiology: CB Mercuray, NewTom 3G and i-CAT. Dentomaxillofac Radiol 35 (2006): 219-26.

[4] Ludlow, J. B. and Ivanovic, M. Comparative dosimetry of dental CBCT devices and 64-slice CT for oral and maxillofacial radiology. Oral Surg Oral Med Oral Pathol Oral Radiol Endod 106 (2008): 106-14.

[5] White, S. C. and Pharoah, M. J. The evolution and application of dental maxillofacial imaging modalities. Dent Clin North Am 52 (2008): 689-705.

[6] Hirsch, E., Wolf, U., Heinicke, F. and Silva, M. A. Dosimetry of the cone beam computed tomography Veraviewepocs 3D compared with the 3D Accuitomo in different fields of view. Dentomaxillofac Radiol 37 (2008): 268-73.

[7] Pauwels, R., et al. Effective dose range for dental cone beam computed tomography scanners. Eur J Radiol 81 (2012): 267-71.

[8] Gilmore, J., Weldon, J., Lares, M. and Hamamatsu Corp. CMOS technology for digital dental imaging. BioPhotonics [Online]. 2010. Available from: http://www.photonics.com/Article.aspx?AID=42008 [2013, Oct 20]

[9] IAEA. Dosimetry in diagnostic radiology: an international code of practice. TRS No 457. Vienna: IAEA Publishing Section, 2007, pp. 25-28.

[10] European Commission. European guidelines on quality criteria for computed tomography. EUR 16262 EN. Luxembourg: Office for Official Publications of the European Communities, 1999, p. 70.

[11] ICRP Publication 60. 1990 Recommendations of the International Commission on Radiological Protection. Annals of the ICRP 21 (1991): 1-201.

[12] ICRP Publication 103. The 2007 Recommendations of the International Commission on Radiological Protection. ICRP publication 103. Annals of the ICRP 37 (2007): 1-332.

[13] Lofthag-Hansen, S., Thilander-Klang, A., Ekestubbe, A., Helmrot, E. and Grondahl, K. Calculating effective dose on a cone beam computed tomography

device: 3D Accuitomo and 3D Accuitomo FPD. Dentomaxillofac Radiol 37 (2008): 72-9.

[14] J. MORITA Mfg. Corp. 3D Accuitomo 170 Brochure [Online]. Available from: http://www.morita.com [2012, Oct 30]

[15] Carestream health Inc. The complete guide to KODAK Dental Systems product [Online]. Available from: http://3.imimg.com/data3/XF/ED/MY-1466831/kodak-rvg-6100-digital-radiography-system.pdf [2012, Oct 30]

[16] Carestream health Inc. KODAK 9500 Cone Beam 3D System User Guide (SM717)_Ed 01 [Online]. Available from: http://www.carestreamdental.com [2012, Oct 30]

[17] Araki, K., Patil, S., Endo, A. and Okano, T. Dose indices in dental cone beam CT and correlation with dose area product. Dentomaxillofac Radiol (2013): 20120362.

[18] Pauwels, R., et al. Dose distribution for dental cone beam CT and its implication for defining a dose index. Dentomaxillofac Radiol 41 (2012): 583-93.

[19] Lukat, T. D., Wong, J. C. and Lam, E. W. Small field of view cone beam CT temporomandibular joint imaging dosimetry. Dentomaxillofac Radiol 42 (2013): 20130082.

[20] Endo, A., Katoh, T., Vasudeva, S., Kobayashi, I. and Okano, T. A preliminary study to determine the diagnostic reference level using dose-area product for limited-area cone beam CT. Dentomaxillofac Radiol 42 (2013): 20120097.

[21] Holroyd, J. and Walker, A. Recommendations for the design of x-ray facilities and the quality assurance of dental cone beam CT (computed tomography) systems. A report of the HPA working party on dental cone beam CT. HPA-RDP-065. Chilton: Health Protection Agency, 2010, pp. 9-12.

จุฬาลงกรณ์มหาวิทยาลัย
Chulalongkorn University

APPENDICES

จุฬาลงกรณ์มหาวิทยาลัย
Chulalongkorn University

Appendix A: Data record form

1. Data record form of 3D Accuitomo 170

Table A1: Data record form of 3D Accuitomo 170

Type of FOVs	FOVs (diameter (cm) x height (cm))	C_{VOL} (mGy)	DLP (mGy.cm)	E (μSv)	E x 2 (μSv)	E x 3 (μSv)
Small FOV	4x4					
	6x6					
Medium FOV	8x8				-	-
	10x5				-	-
	10x10				-	-
	14x5				-	-
	14x10				-	-
	17x5				-	-
Large FOV	17x12				-	-

2. Data record form of Kodak 9000 3D and Kodak 9500 CB 3D

Table A2: Data record form of Kodak 9000 3D and Kodak 9500 CB 3D

Type of FOVs	FOVs	DAP ($mGy.cm^2$)	DAPx2 ($mGy.cm^2$)	DAPx3 ($mGy.cm^2$)
Small FOV (diameter (cm) x height (cm))	5 x 3.7			
Multi-small FOV (W x D x H (cm^3))	9.3 x 5 x 3.7		-	-
	9.3 x 7.4 x 3.7		-	-
Medium FOV (diameter (cm) x height (cm))	15 x 9		-	-
Large FOV (diameter (cm) x height (cm))	20.6 x 18		-	-

Appendix B: Quality control of the CBCT scanner – 3D Accuitomo170 FPD XYZ Slice View Tomograph

1. kVp accuracy

Purpose: To evaluate accuracy of measured kVp and set kVp.

Method:
- Place dosimeter at center of rotation and choose field size 10x10cm^2.
- Vary kVp from 60-90 in step of 10, set mA at 5 and 1 second, mAs is 5.
- Record measured kVp and exposure (mGy).
- Calculate tube output (mGy/mAs).
- Plot graph of linearity of set and measured kVp and kVp vs tube output (mGy/mAs).

Tolerance: The difference between the set and measured kVp should not exceed 5 kVp or the percent kVp deviation should not exceed 10% of set kVp

Results:

Table B1: kVp accuracy for the set and measured values

Set kVp	Measured kVp	% kVp Dev.	mGy	mGy/mAs
60	59.64	-0.60	0.185	0.04
70	69.75	-0.36	0.261	0.05
80	80.82	1.02	0.351	0.07
90	90.67	0.74	0.445	0.09

จุฬาลงกรณ์มหาวิทยาลัย
CHULALONGKORN UNIVERSITY

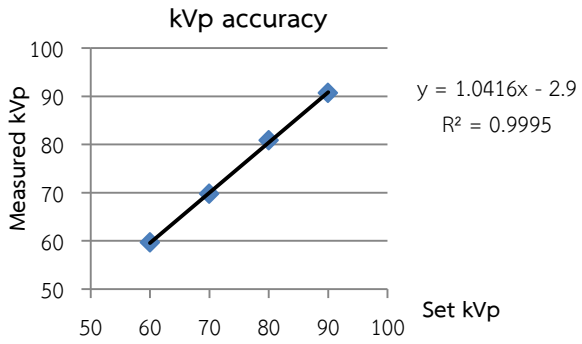

Figure B1: The linearity of set and measured kVp with R^2 of 0.9995

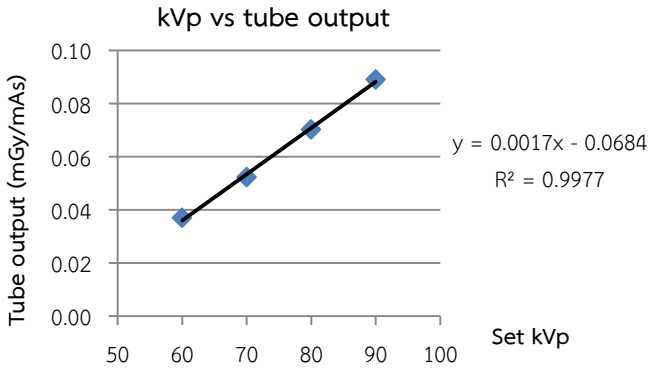

Figure B2: The linearity of set kVp and tube output with R^2 of 0.9977

Comment: Absolute values of % kVp deviation range from 0.36-1.02%.

PASS

จุฬาลงกรณ์มหาวิทยาลัย
Chulalongkorn University

2. mAs linearity

Purpose: To determine the response of the tube output with increasing mAs.

Method: -Place dosimeter at center of rotation.

- Vary mAs from 1-10 in steps of 5, set 90 kVp and 17.5 seconds.

- Record the exposure (mGy).

- Calculate tube output (mGy/mAs).

- Calculate mean, SD and coefficient of variation (CV) of tube output.

- Plot graph of mAs linearity.

Tolerance: Coefficient of variation should not exceed 0.1.

Results:

Table B2: The linearity of mAs with mGy/mAs

mA	mAS	mGy	mGy/mAs	C.V.
1	17.5	0.0995	0.0057	
5	87.5	0.4450	0.0051	0.0557
10	175	0.8530	0.0049	0.0212

SD = 0.0004

Mean = 0.0052

CV = 0.08

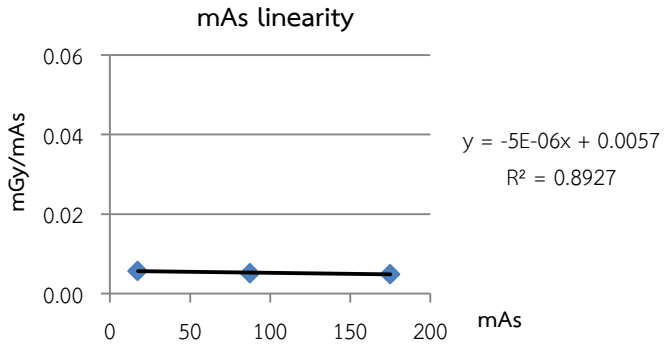

Figure B3: The linearity of mAs and mGy/mAs with R^2 of 0.8927

Comment: Coefficient of variation is 0.08.

PASS

3. $C_{a,100}$

Purpose: To measure $C_{a,100}$

Dosimeter: Unfors Xi CT detector

Method: - Place the dosimeter at center of rotation (54 cm from x-ray source).

- Set 80kVp, 5mA and 17.5 seconds for every FOVs.

- Record the exposure.

Results:

Table B3: $C_{a,100}$ of every FOVs of 3D Accuitomo 170

FOV	Air Kerma1 (mGy)	Air Kerma2 (mGy)	Air Kerma3 (mGy)	Average Air Kerma (mGy)	Tube output (mGy/mAs)
4x4	5.797	5.779	5.794	5.79	0.07
10x5	7.61	7.61	7.61	7.61	0.09
14x5	7.838	7.822	7.827	7.83	0.09
17x5	8.4	8.406	8.4	8.40	0.10
6x6	8.735	8.728	8.737	8.73	0.10
8x8	11.43	11.41	11.45	11.43	0.13
10x10	12.73	12.74	12.74	12.74	0.15
14x10	12.74	12.72	12.74	12.73	0.15
17x12	13.26	13.24	13.247	13.25	0.15

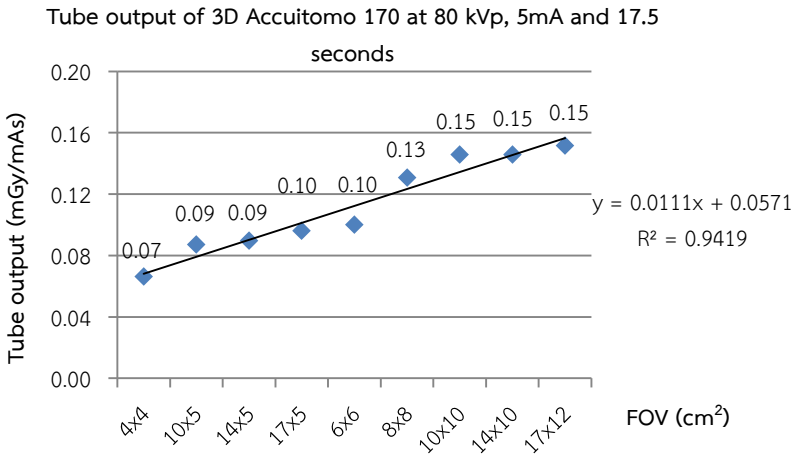

Figure B4: Tube output of various FOVs of 3D Accuitomo 170 with R^2 of 0.9419

4. CT dose index

Purpose: To compare measured and system manual CT dose index values

Tolerance: Measured CT dose index should be within ±30% from system manual.

4.1. C_{VOL}

Method: - Place PMMA 16 cm diameter phantom at the center of rotation

- Set 90kVp, 5mA and 17.5 seconds

- Measure CTDI center and CTDI peripheral (4 points) (figure B5)

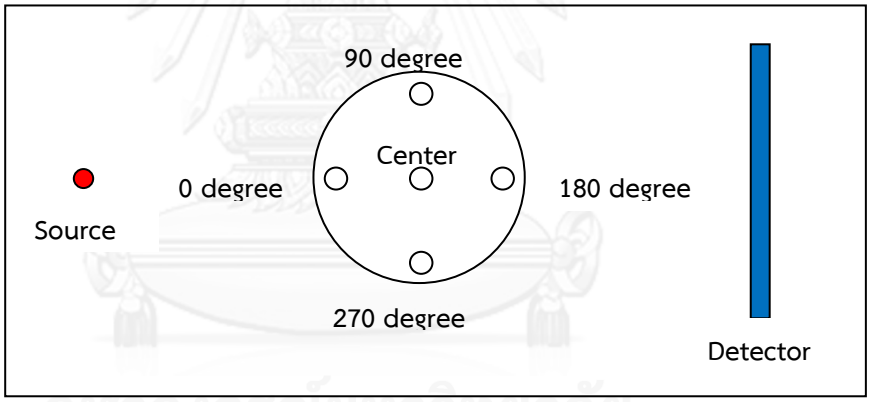

Figure B5: Position of ionization chamber

สถาบันวิทยบริการ
CHULALONGKORN UNIVERSITY

- Calculate C_W and C_{VOL}

- Compare the calculated and system manual C_{VOL}

Table B4: CTDI at 90kVp, 5mA and 17.5 seconds

Acquisition (cm^2)	scan mode	CT Dose Index (mGy)							
		CTDI center	0	90	180	270	CTDI peripheral	C_W	C_{VOL}
4x4	360	2.553	1.435	1.191	1.421	1.034	1.27	1.70	1.70
6x6	360	4.365	2.964	2.445	2.927	2.773	2.78	3.31	3.31
10x10	360	7.287	6.292	5.459	6.369	6.098	6.05	6.47	6.47
17x12	360	8.064	7.927	6.411	7.513	7.939	7.45	7.65	7.65

Table B5: Comparison of measured and system manual C_{VOL} values

Acquisition (cm^2)	scan mode	C_W or C_{VOL}	C_{VOL} from manual	Different values	% deviation
4x4	360	1.70	4.6	2.9	63%
6x6	360	3.31	5.7	2.39	42%
10x10	360	6.47	6.9	0.43	-6.23%
17x12	360	7.65	8.7	1.05	-12.03%

Comment: Absolute value of % deviation of FOVs 10x10 and 17x12 cm^2 are 6.23 and 12.03% respectively.

PASS

The differences between measured and system manual C_{VOL} result from uncertainties of phantom and ionization chamber positioning. Measured C_{VOL} from FOVs 4x4 and 6x6 cm^2 are not acceptable because the ionization chamber at peripheral site of phantom was outside the primary beam and the dose distribution across the FOV is non uniform.

จุฬาลงกรณ์มหาวิทยาลัย
Chulalongkorn University

4.2. CTDI center at various tube current

Method: - Place PMMA 16 cm diameter phantom at the center of rotation.

- Select FOV 10x10cm^2 with scan mode 360°.

- Set 90kVp and 17.5 seconds.

- Measure CTDI center at various tube current; 1, 5, 10mA.

- Normalize CTDI center.

Table B6: Normalized CTDI center at 90kVp, 17.5 seconds and various tube currents normalized CTDI to 5 mA

Tube current (mA)	CTDI center (mGy)	Normalized CTDI center		% Dev.
		from measurement	from system manual	
1	1.55	0.21	0.21	0
5	7.29	1	1	0
10	14.23	1.95	1.95	0

Comment: Normalized CTDI center in this study is the same as normalized CTDI from system manual.

4.3. CTDI peripheral at various tube potential

Method: - Place PMMA 16 cm diameter phantom at the center of rotation.

- Select FOV 4x4 and 10x10cm^2 and scan mode 360°.

- Set 5mA and 17.5 seconds.

- Measure CTDI peripheral at various kVp from 60-90kVp in steps of 10kVp.

- Normalize CTDI peripheral.

จุฬาลงกรณ์มหาวิทยาลัย
Chulalongkorn University

Table B7: CTDI peripheral at 60kVp, 5mA and 17.5 seconds

Acquisition FOV(cm^2)	scan mode	CT dose index				
		0	90	180	270	CTDI peripheral
4x4	360	0.09	0.35	0.42	0.40	0.32
10x10	360	2.21	1.84	2.20	2.12	2.09

Table B8: CTDI peripheral at 70kVp, 5mA and 17.5 seconds

Acquisition FOV(cm^2)	**scan mode**	**CT dose index**				
		0	90	180	270	CTDI peripheral
4x4	360	0.14	0.56	0.62	0.59	0.48
10x10	360	3.35	2.84	3.37	3.23	3.20

Table B9: CTDI peripheral at 80kVp, 5mA and 17.5 seconds

Acquisition FOV(cm^2)	scan mode	CT dose index				
		0	90	180	270	CTDI peripheral
4x4	360	0.20	0.79	0.85	0.81	0.66
10x10	360	4.75	4.08	4.80	4.59	4.55

Table B10: CTDI peripheral at 90kVp, 5mA and 17.5 seconds

Acquisition FOV(cm^2)	scan mode	CT dose index				
		0	90	180	270	CTDI peripheral
4x4	360	1.435	1.191	1.421	1.034	1.27
10x10	360	6.292	5.459	6.369	6.098	6.05

Table B11: Normalized CTDI peripheral at 5mA, 17.5 seconds and various kVp normalized CTDI to 90 kVp

FOV (cm^2)	kVp	Normalized CTDI peripheral		Different values
		from measurement	from manual	
4x4	60	0.25	0.38	-0.13
	70	0.38	0.56	-0.18
	80	0.52	0.77	-0.25
	90	1	1	0.00
10x10	60	0.35	0.37	-0.02
	70	0.53	0.55	-0.02
	80	0.75	0.77	-0.02
	90	1	1	0.00

Comment: The measured CTDI were almost less than the manual values according to the various uncertainties such as position of phantom and ionization chamber, environment and etc.

5. Spatial resolution test

Purpose: To ensure that the spatial resolution of a reconstructed image comply with manufacturer's standard.

Method: - Place wire phantom (PMMA tube 5cm diameter with vertical 0.1mm stainless steel wire) on the table.

- Select FOV 4x4cm^2.

- Acquire image at 60kVp, 1mA and 17.5 seconds.

- Analyze the image using A3dxImageQA software.

Tolerance: MTF value at 2 lp/mm is more than 10%.

Result: MTF value at 2 lp/mm is 13.3%.

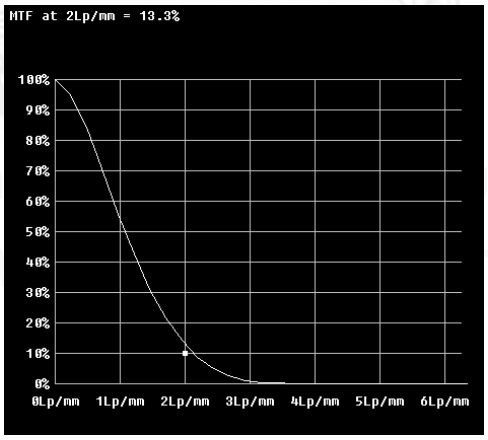

Figure B6: The relation of MTF and line pairs/mm

Comment: **PASS**

6. Noise, Uniformity/Grayscale and contrast resolution test

Purpose: SD values of grayscale and noise comply with the manufacturer's specifications.

For contrast resolution, four different materials show different ROI values.

Method: -Place contrast phantom (PMMA cylinder 5cm diameter with air, PMMA, bone equivalent plastic and aluminum blocks at center axis) on the table by putting the air side up and aluminum side down.

- Select FOV 4x4cm^2.

- Acquire image at 70kVp, 1mA and 17.5 seconds.

- Analyze the image using A3dxImageQA software.

Tolerance: Gray scale (SD of 5 means) and noise (SD at A) value in axial slice of acrylic part should be less than 12.5.

For contrast resolution, ROI value of each material should not overlap each other.

Results: Gray scale (SD of 5 means) = 1.23 (Figure B7)

Noise (SD at A) = 3.51 (Figure B7)

ROI value didn't overlap each other (Figure B8)

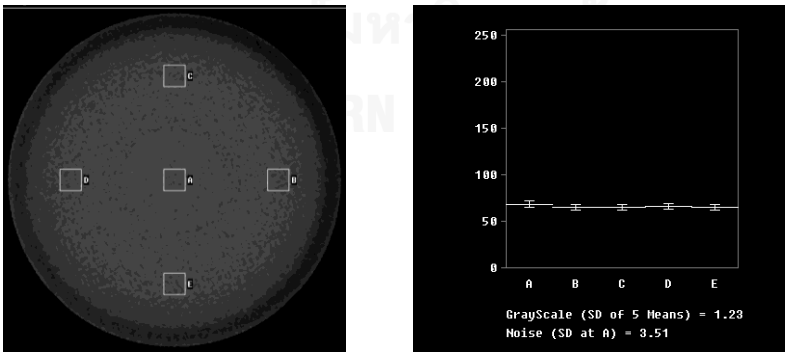

a b

Figure B7: Axial slice of the plain acrylic part with 5 ROIs (a) and noise, uniformity/grayscale graph (b)

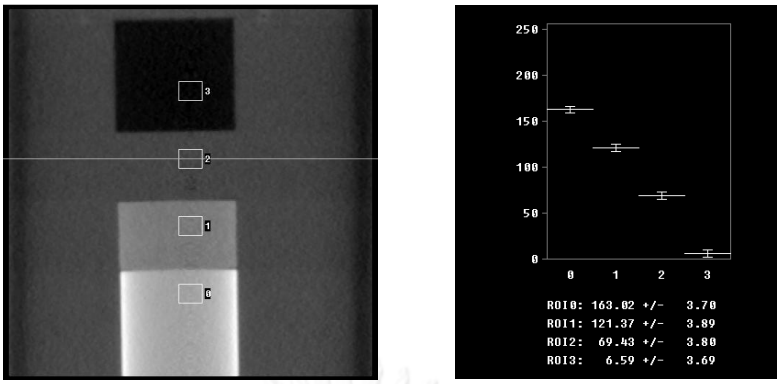

a b

Figure B8: Contrast scale ROI of four different materials (a) and contrast scale graph (b)

Comment: **PASS**

7. Artifact test

Purpose: To test for image artifacts.

Method: **-** Place 3D phantom horizontally on the table.

- Select FOV 4x4cm^2.

- Acquire image at 70kVp, 1mA and 17.5 seconds.

- Using “i-Dixel” software.

Tolerance: 1) No significant distortion along the straight and round parts of the mushroom that can affect clinical diagnosis.

2) No significant distortion at the edge of the mushroom that can affect clinical diagnosis.

3) No virtual image around the mushroom image that can affect clinical diagnosis.

Result: Figure B9 shows neither distortion nor artifact in the mushroom image.

จุฬาลงกรณ์มหาวิทยาลัย
Chulalongkorn University

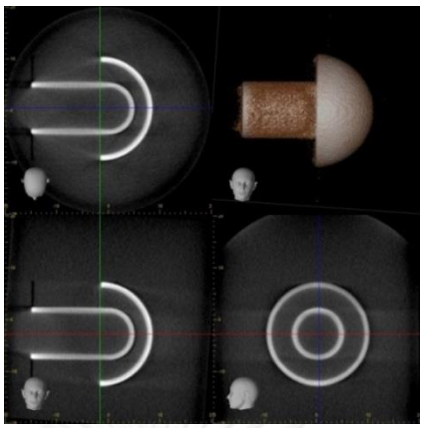

Figure B9: Mushroom image for artifact test

Comment: **PASS**

8. Patient position test

Purpose: To evaluate accuracy of the patient position.

Method: -Place the 3D phantom with cap side up on the table.

- Select FOV 4x4cm^2.

- Acquire image at 70kVp, 1mA and 17.5 seconds.

- After reconstruction, move green and blue lines to the center of the mushroom cap in z plane and red line to the bottom edge of the cap in X, Y planes.

- Using "i-Dixel" software.

Tolerance: XYZ values of the slice position should be within $\pm$ 2mm.

Result: Green line (X) is 0.5mm out of center.

Blue line (Y) is 0mm out of center.

Red line (Z) is about 1.5mm out of center.

จุฬาลงกรณ์มหาวิทยาลัย
Chulalongkorn University

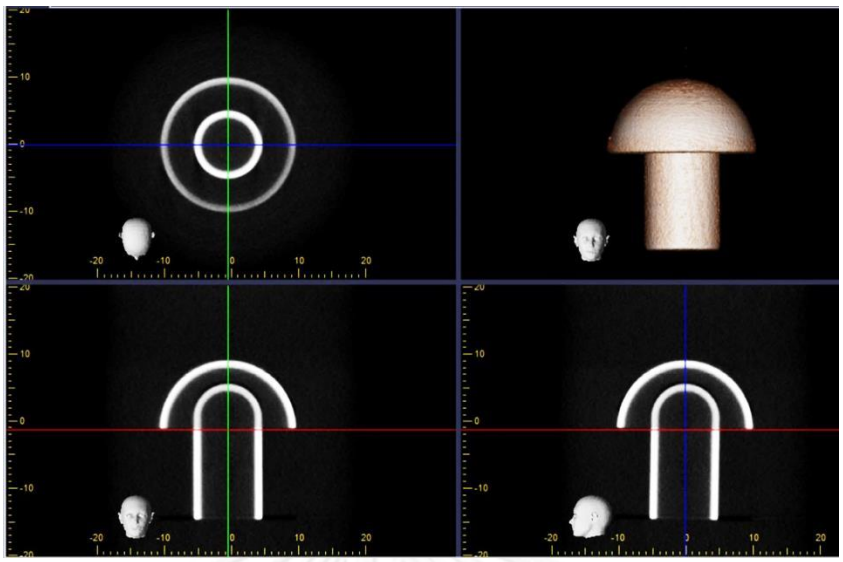

Figure B10: Mushroom image for patient position test

Comments: XYZ values - **PASS**.

จุฬาลงกรณ์มหาวิทยาลัย
Chulalongkorn University

Appendix C: Quality control of the CBCT scanner – Kodak 9000 3D

1. kVp accuracy

Purpose: To evaluate the accuracy of measured and set kVp.

Method:
- Place dosimeter at center of rotation.
- Vary kVp from 60-90 in step of 10 and set mA at 5 and 10.8seconds, mAs is 54.
- Record measured kVp and exposure (mGy).
- Calculate tube output (mGy/mAs).
- Plot graph of linearity of set and measured kVp and kVp vs tube output (mGy/mAs).

Tolerance: The difference between the set and measured kVp should not exceed 5 kVp or the percent kVp deviation should not exceed 10% of set kVp

Results:

Table C1: kVp accuracy for the set and measured values

Set kVp	measured kVp	% kVp Dev.	mGy	mGy/mAs	DAP (mGy.cm^2) from monitor
60	57.66	-3.90	0.73	0.013	83.6
70	65.63	-6.24	0.94	0.017	109
80	74.89	-6.39	1.14	0.021	131
90	81.91	-8.99	1.30	0.024	150

จุฬาลงกรณ์มหาวิทยาลัย
Chulalongkorn University

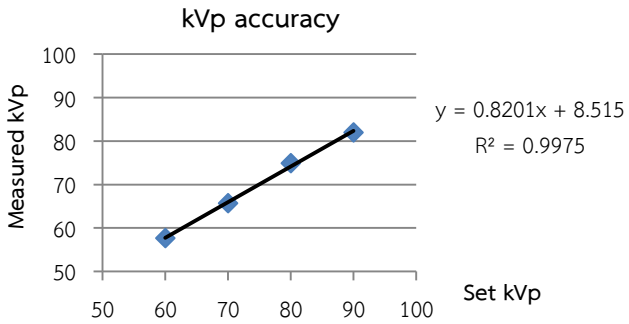

Figure C1: The linearity of set and measured kVp with R^2 of 0.9975

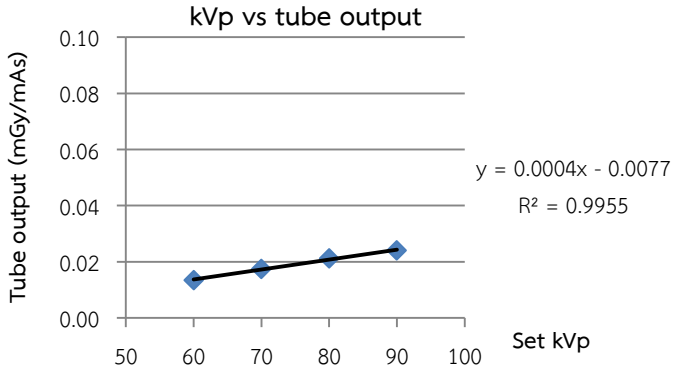

Figure C2: The linearity of set kVp and tube output with R^2 of 0.9955

Comment: Absolute values of % deviation vary from 3.90-8.99%.

PASS

จุฬาลงกรณ์มหาวิทยาลัย
Chulalongkorn University

2. mAs linearity

Purpose: To determine the effect on tube output when increasing mAs.

Method: -Place dosimeter at center of rotation.

- Vary mAs (3.2, 5, 8, 10) and set kVp at 80 and 10.8seconds.

- Record the exposure (mGy).

- Calculate tube output (mGy/mAs).

- Calculate mean, SD and coefficient of variation (CV) of tube output.

- Plot graph of mAs linearity.

Tolerance: Coefficient of variation should not exceed 0.1.

Results:

Table C2: The linearity of mAs with mGy/mAs

mA	mAs	mGy	mGy/mAs	C.V.	DAP ($mGy.cm^2$) from monitor
3.2	34.6	1.432	0.041		83.7
5.0	54.0	2.263	0.042	0.006	131
8.0	86.4	4.324	0.050	0.089	209
10.0	108.0	5.449	0.050	0.004	261

SD = 0.0005
Mean = 0.004
CV = 0.1

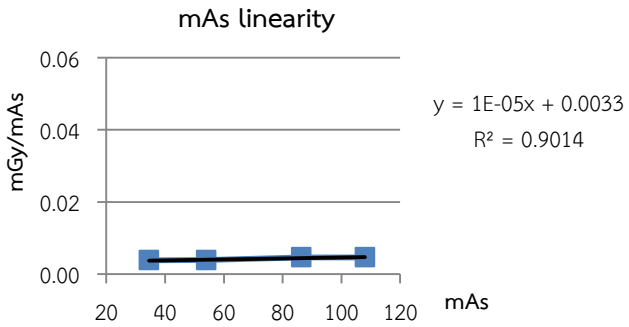

CHULALONGKORN UNIVERSITY

Figure C3: The linearity of mAs and mGy/mAs with R^2 of 0.9014

Comment: Coefficient of variation = 0.1.

PASS

3. $C_{a,100}$

Purpose: To measure $C_{a,100}$

Dosimeter: Unfors Xi CT detector

Method:
- Place the dosimeter at center of rotation (44 cm from x-ray source).
- Set various kVp, mA (as shown in table C3) and 10.8 seconds.
- Record the exposure.

Results:

Table C3: $C_{a,100}$ and tube output of Kodak 9000 3D with various kVp and mAs

Patient size	kVp	mA	FOV	Air Kerma1	Air Kerma2	Air Kerma3	Average Air Kerma (mGy)	Tube output (mGy/mAs)
medium	68	6.3	5x3.7	3.820	3.869	3.843	3.84	0.056
small	70	8	5x3.7	5.163	5.179	5.160	5.17	0.060
child	70	10	5x3.7	6.484	6.506	6.491	6.49	0.060
large	74	10	5x3.7	6.963	6.970	7.006	6.98	0.065
large	80	5	5x3.7	3.858	3.839	3.845	3.85	0.071

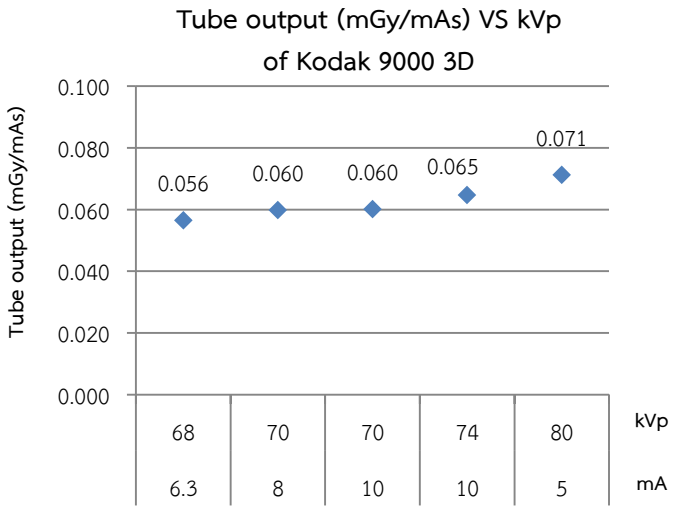

Figure C4: Tube output vs kVp of Kodak 9000 3D

4. Dose area product

Purpose: To compare measured and system manual value of DAPs.

To confirm, for selected scan protocols, the accuracy of the displayed DAP ($mGy.cm^2$) values on the monitor.

Dosimeter: DAP meter: PTW Freiburg Model Diamentor E

Method: - Place the dosimeter at x-ray source side.

- Choose the patient size in program and set parameters (the same as shown in system manual) as the followings:

  - Large size: 68kVp, 6.3mA
  - Medium size: 70kVp, 8mA
  - Small size: 70kVp, 10mA
  - Child size: 74kVp, 10mA

- Expose one (10.8 seconds), two (21.6 seconds) and three volumes (32.4 seconds).

  - One volume: FOV (∅ x H) 5x3.7 cm^2
  - Two volumes: FOV (W x D X H) 9.3x5x3.7 cm^3
  - Three volumes: FOV (W x D X H) 9.3x7.4x3.7cm^3

- Record DAP values.

- Compare measured and system manual value of DAPs.

- Compare DAP from monitor with DAP value from system manual.

Tolerance: Doses should be within ±30% from system manual.

จุฬาลงกรณ์มหาวิทยาลัย
CHULALONGKORN UNIVERSITY

Results:

Table C4: Comparison of measured and system manual DAP values

Patient size	kVp	mA	volume	DAP (mGy.cm^2) from measurement	DAP (mGy.cm^2) from manual	%deviation
Large	68	6.3	One	130	131	0.76
			Two	260	263	1.14
			Three	390	394	1.02
Medium	70	8	One	170	175	2.86
			Two	350	349	0.29
			Three	520	524	0.76
Small	70	10	One	210	218	3.67
			Two	440	436	0.92
			Three	650	654	0.61
Child	74	10	One	230	235	2.13
			Two	470	471	0.21
			Three	700	706	0.85

Table C5: Comparison of DAP from monitor with DAP value from system manual

Patient size	kVp	mA	volume	DAP (mGy.cm^2) from monitor	DAP (mGy.cm^2) from manual	% deviation
large	68	6.3	One	131	131	0.00
			Two	262	263	0.38
			Three	394	394	0.00
medium	70	8	One	174	175	0.57
			Two	348	349	0.29
			Three	523	524	0.19
small	70	10	One	218	218	0.00
			Two	435	436	0.23
			Three	653	654	0.15
child	74	10	One	236	235	0.43
			Two	472	471	0.21
			Three	708	706	0.28

จุฬาลงกรณ์มหาวิทยาลัย
Chulalongkorn University

Comments: Absolute values of % deviation between measured and system manual DAP values are in the range of 0.21-3.67, **PASS**.

Absolute values of % deviation between DAP from monitor with DAP from system manual vary from 0.00-0.57, **PASS**.

5. Rotative arm axis

Purpose: To check the rotative arm axis.

Method: - Place tool base on the chin rest base.

- Position the testing tubes and the metal rod on the tool base.

- Raise the chin rest base to the maximum height.

- Acquire an image at 60kVp, 2mA and 10.8 seconds.

- Adjust appropriate contrast of the image.

Tolerance: - Acquire image that displays 3 circles is satisfactory.

Result:

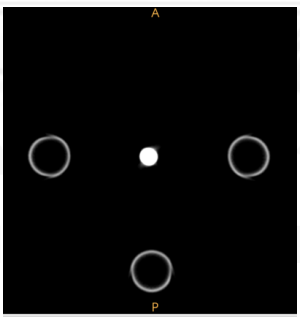

Figure C5: Axial view of metal rod and tubes

Comment: - Image is satisfactory.

PASS

6. Spatial linearity

Purpose: To verify spatial linearity by measuring the distance between pin points (center to center) compare with known distance (50mm).

Method: -Place CATPHAN® 600 in upright position.

- Acquire an image of section CTP 404 at 90kVp, 10mA and 10.8seconds.

- Measure the distance between Teflon pins.

Tolerance: Difference between measured and known distance should be within ±0.5mm.

Result: -Distance between Teflon is 49.7mm.

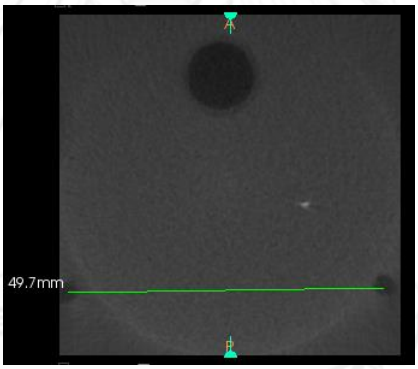

Figure C6: Measurement of distance between Teflon pins

จุฬาลงกรณ์มหาวิทยาลัย
Chulalongkorn University

Comment: - Measured distance is 0.3mm different from actual distance (50mm).

PASS

7. MTF measurement

Purpose: To ensure that the spatial resolution of a reconstructed image comply with manufacturer's standard.

Method: -Place CATPHAN® 600 in upright position.

- Acquire an image of section CTP 591 at 90kVp, 10mA and 10.8seconds.

- Measure MTF by Image J.

Tolerance: - The value of the Modulation Transfer Function (MTF) at 10% is superior to 1 lp/mm.

Result: - MTF at 10% is 2.5 lp/mm

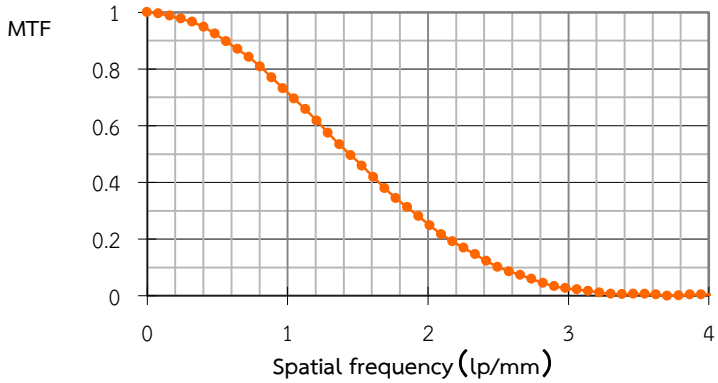

Figure C7: Modulation transfer function VS spatial frequency graph

Comment: PASS

จุฬาลงกรณ์มหาวิทยาลัย
Chulalongkorn University

Appendix D: Quality control of the CBCT scanner – Kodak 9500 Cone Beam 3D

1. kVp accuracy

Purpose: To evaluate the accuracy of measured and set kVp.

Method: -Place dosimeter at center of rotation.

- Select FOV 15x9cm^2

  - Vary kVp from 70-90 in steps of 10 and set mA at 5 and 10.8seconds, mAs is 54.

- Select FOV 20.6x18cm^2

  - Vary kVp from 70-90 in steps of 10 and set mA at 5 and 10.8seconds, mAs is 54.

- Record the exposure (mGy) and displayed kVp.

- Calculate tube output (mGy/mAs).

- Plot graph of linearity of set and measured kVp and kVp vs tube output (mGy/mAs).

Tolerance: The difference between the set and measured kVp should not exceed 5 kVp or the percent kVp deviation should not exceed 10% of set kVp

จุฬาลงกรณ์มหาวิทยาลัย
Chulalongkorn University

Results:

Table D1: kVp accuracy for the set and measured values of medium FOV (FOV 15x9cm^2)

Set kVp	measured kVp	% kVp Dev.	mGy	mGy/mAs	DAP (mGy.cm^2) from monitor
70	68.79	-1.73	0.10	0.002	135
80	78.09	-2.39	0.20	0.004	211
90	88.92	-1.20	0.32	0.006	302

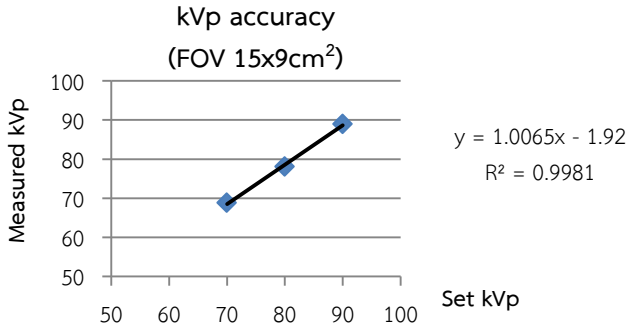

Figure D1: The linearity of set and measured kVp with R^2 0.9981 of medium FOV (FOV 15x9cm^2)

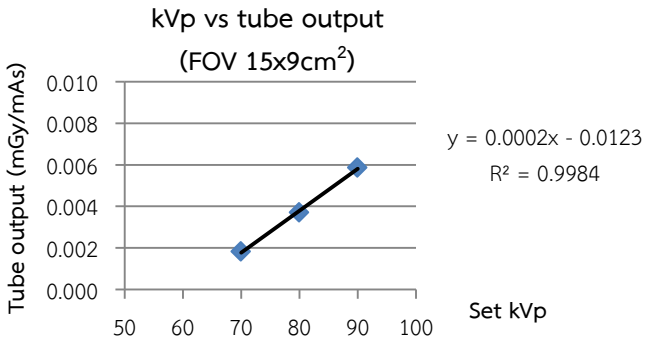

Figure D2: The linearity of set kVp and tube output with R^2 0.9984 of medium FOV (FOV 15x9cm^2)

Table D2: kVp accuracy for the set and measured values of large FOV (FOV 20.6x18cm^2)

Set kVp	measured kVp	% kVp Dev.	mGy	mGy/mAs	DAP (mGy.cm^2) from monitor
70	67.22	-3.97	0.09	0.002	313
80	76.57	-4.29	0.23	0.004	502
90	84.96	-5.60	0.37	0.007	733

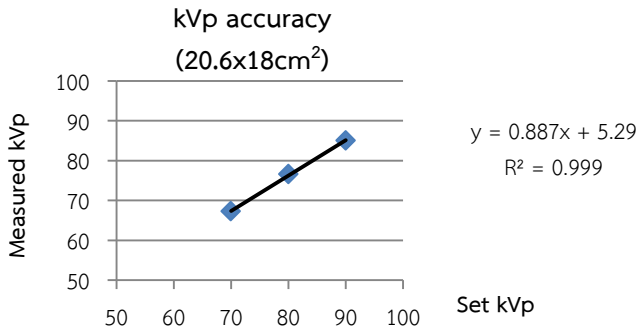

Figure D3: The linearity of set and measured kVp with R^2 of 0.999 of large FOV (FOV 20.6x18cm^2)

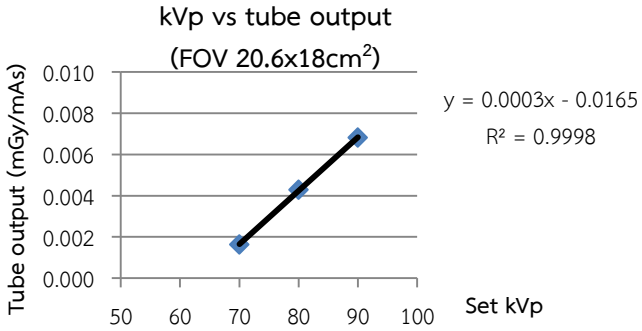

Figure D4: The linearity of set kVp and tube output with R^2 of 0.9998 of large FOV (FOV 20.6x18cm^2)

จุฬาลงกรณ์มหาวิทยาลัย
Chulalongkorn University

Comment: For FOV 15x9cm^2, absolute values of % kVp deviation vary from 1.2-2.39%.

For FOV 20.6x18cm^2, absolute values of % kVp deviation vary from 3.97-5.60%.

PASS

2. mAs linearity

Purpose: To determine the response of the tube output with increasing mAs.

Method: - Place dosimeter at center of rotation.

- Vary mAs (3.2, 5, 8, 10mAs) and set at 80kVp and 10.8seconds.

- Record the exposure (mGy).

- Calculate tube output (mGy/mAs).

- Calculate mean, SD and coefficient of variation (CV) of tube output.

- Plot graph of mAs linearity.

Tolerance: Coefficient of variation should not exceed 0.1.

Results:

Table D3: The linearity of mAs with mGy/mAs of medium FOV (FOV 15x9cm^2)

mA	mAs	mGy	mGy/mAs	C.V.	DAP (mGy.cm^2) from monitor
3.2	34.6	0.53	0.0154		135
5.0	54.0	0.85	0.0158	0.011	211
8.0	86.4	1.38	0.0159	0.004	337
10.0	108.0	1.72	0.0160	0.001	421

จุฬาลงกรณ์มหาวิทยาลัย
Chulalongkorn University

SD = 0.00002
Mean = 0.0015
CV = 0.01

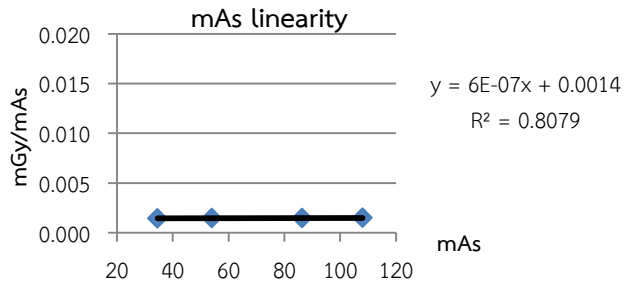

Figure D5: The linearity of mAs and mGy/mAs with R^2 of 0.8079 of medium FOV (FOV 15x9cm^2)

Table D4: The linearity of mAs with mGy/mAs of large FOV (FOV 20.6x18cm^2)

mA	mAs	mGy	mGy/mAs	C.V.	DAP (mGy.cm^2) from monitor
3.2	34.6	0.5946	0.017		321
5.0	54.0	0.9325	0.017	0.004	502
8.0	86.4	1.506	0.017	0.005	804
10.0	108.0	1.877	0.017	0.001	1004

SD = 0.00001
Mean = 0.0016
CV = 0.01

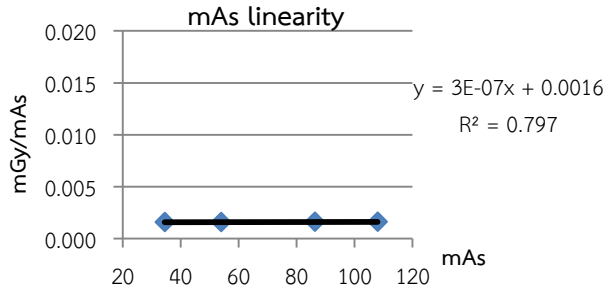

Figure D6: The linearity of mAs and mGy/mAs with R^2 of 0.797 of large FOV (FOV 20.6x18cm^2)

Comment: Both FOVs (15x9cm^2, 20.6x18cm^2), coefficient of variations are 0.01.

PASS

3. $C_{a,100}$

Purpose: To measure $C_{a,100}$

Dosimeter: Unfors Xi CT detector

Method: - Place the dosimeter at center of rotation (54 cm from x-ray source).

- Set 80kVp, 5mA and 10.5 seconds for every FOVs and record the exposure.

Results:

Table D5: $C_{a,100}$ and tube output of Kodak 9500 CB 3D

FOV	Air Kerma1	Air Kerma2	Air Kerma3	Average Air Kerma (mGy)	Tube output (mGy/mAs)
15x9	1.550	1.555	1.551	1.55	0.03
20.6x18	1.619	1.609	1.612	1.61	0.03

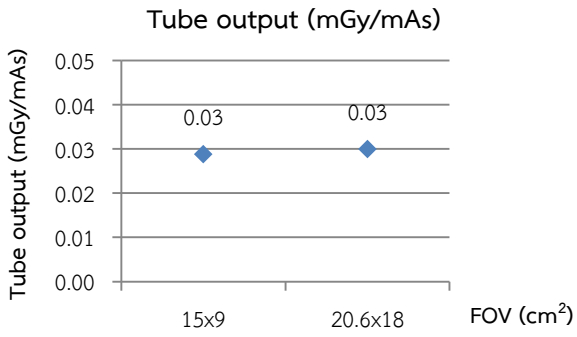

Figure D7: Tube output of Kodak 9500 CB 3D

4. Dose area product

Purpose: To compare measured and system manual value of DAPs.

To confirm, for selected scan protocols, the accuracy of the displayed DAP ($mGy.cm^2$) values on the monitor.

Dosimeter: DAP meter: PTW Freiburg Model Diamentor E

Method: - Place the dosimeter at x-ray source side.

- Set 80kVp, 5mA and 10.8 seconds.

- Record DAP values.

- Compare measured and system manual value of DAPs.

- Compare DAP from monitor with DAP from system manual.

Tolerance: Doses should be within $\pm$30% from system manual.

Results:

Table D6: Comparison of measured and system manual DAP values

FOV (cm^2)	DAP from measurement ($mGy.cm^2$)	DAP from manual ($mGy.cm^2$)	% deviation
15x9	133.33	185	-27.93
20.6x18	296.67	435	-31.80

Table D7: Comparison of DAP value from monitor with DAP value from system manual

FOV (cm^2)	DAP from monitor ($mGy.cm^2$)	DAP from manual ($mGy.cm^2$)	% deviation
15x9	211	185	14.05
20.6x18	502	435	15.40

Comment: - Absolute values of % deviation between measured and system manual DAP values in medium FOV is 27.93%, **PASS**. In large FOV, % deviation is 31.8 %, **FAIL**.

Percent deviation in large FOV exceeds the tolerance because of the uncertainties in position of ionization chamber and external DAP meter was not calibrated for long time.

- Absolute values of % deviation of DAP from monitor compared with DAP from system manual varied from 14.05-15.4%, **PASS**.

จุฬาลงกรณ์มหาวิทยาลัย
Chulalongkorn University

5. Rotative arm axis

Purpose: To check the rotative arm axis.

Method: -Place tool base on the chin rest base.

- Position the testing tubes and the metal rod on the tool base

- Raise the chin rest base to the maximum height.

- Acquire an image for both FOVs (15x9, 20.6x18cm^2) at 60kVp, 2mA and 10.8 seconds.

- Adjust appropriate contrast of the images.

Tolerance: -Acquired image that displays 3 circles is satisfactory.

Results:

a. FOV 15x9cm^2 b. FOV 20.6x18cm^2

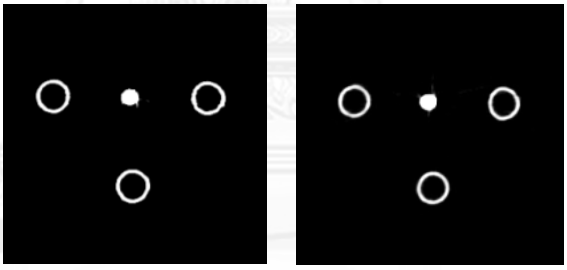

Figure D8: Axial view of metal rod and tubes of medium FOV (a) and large FOV (b)

จุฬาลงกรณ์มหาวิทยาลัย
CHULALONGKORN UNIVERSITY

Comment: Both images are satisfactory.

PASS

6. Circular symmetry and spatial linearity

Purpose: To test for circular symmetry of the CBCT image, including calibration of the CBCT display system.

To verify spatial linearity by measuring diameter of the phantom and the distance between pin points (center to center) compared with known distance.

Method: -Place CATPHAN®600 in upright position.

- Acquire an image of section CTP 404 for both FOVs (15x9, 20.6x18cm^2) at 90kVp, 10mA and 10.8seconds.

- Look at shape of the image.

- Measure diameter of the phantom and the distance between Teflon pins.

Tolerances: Images are circular symmetry.

Difference between measured and known distance should be within ±0.5mm.

Results:

Circular symmetry

a. FOV15x9cm^2 b. FOV 20.6x18cm^2

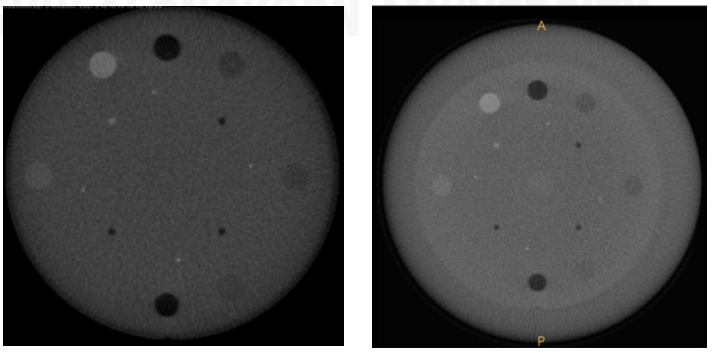

Figure D9: Axial view of circular phantom of medium FOV (a) and large FOV (b)

Spatial linearity

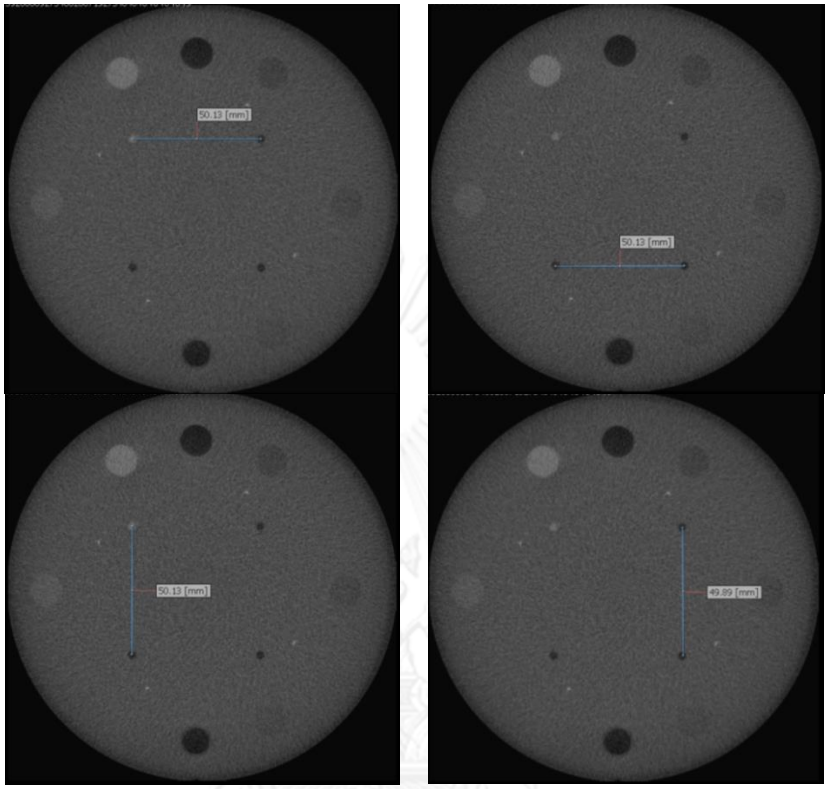

Figure D10: Measurement for distance accuracy between Teflon pins in medium FOV (FOV15x9cm^2)

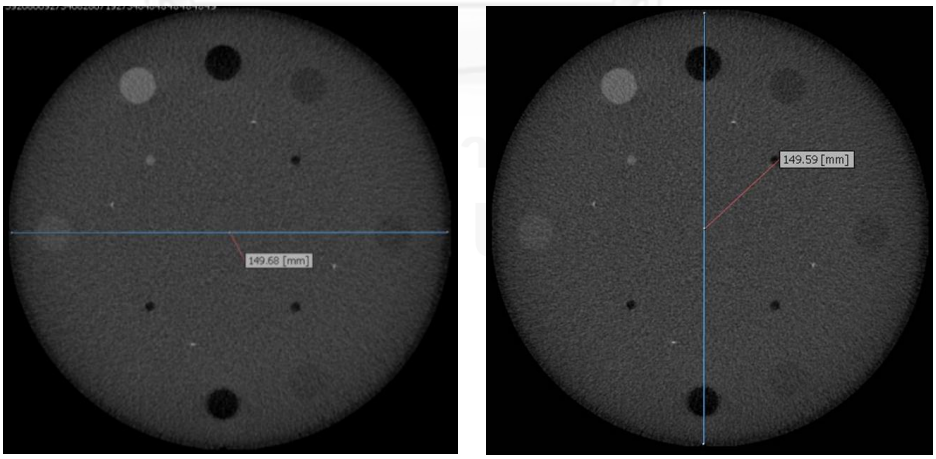

Figure D11: Measurement for diameter distance accuracy in medium FOV (FOV15x9cm^2)

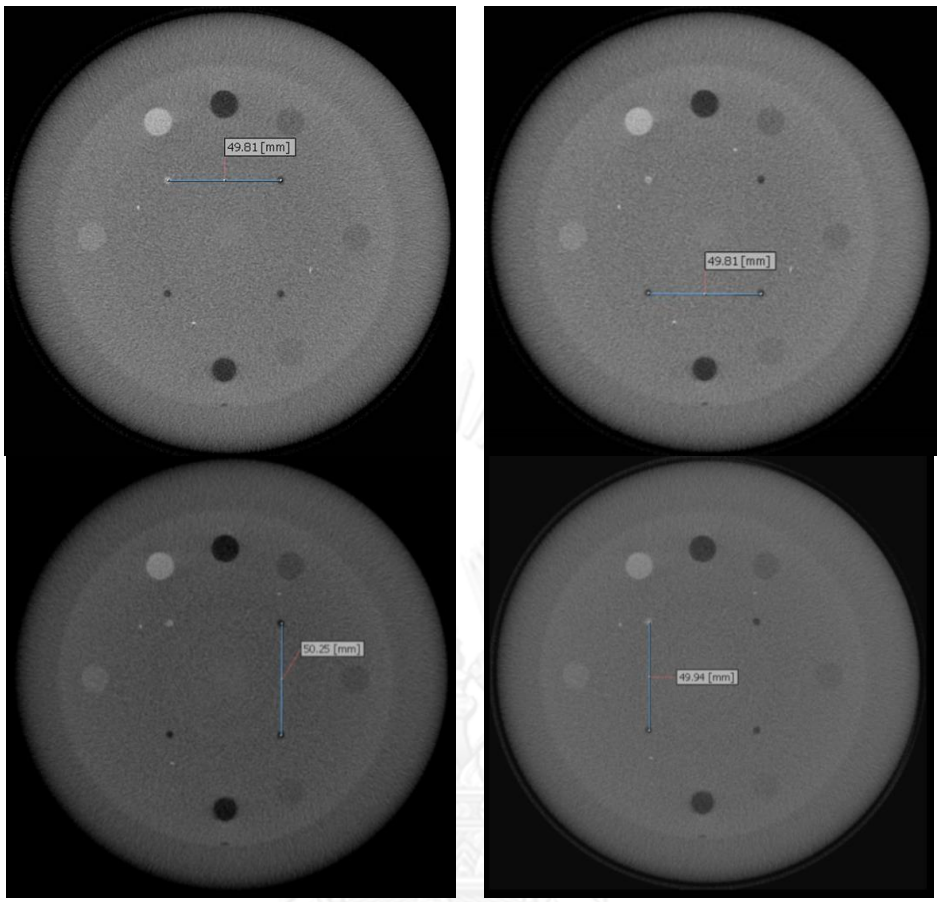

Figure D12: Measurement for distance accuracy between Teflon pins in large FOV (FOV20.6x18cm^2)

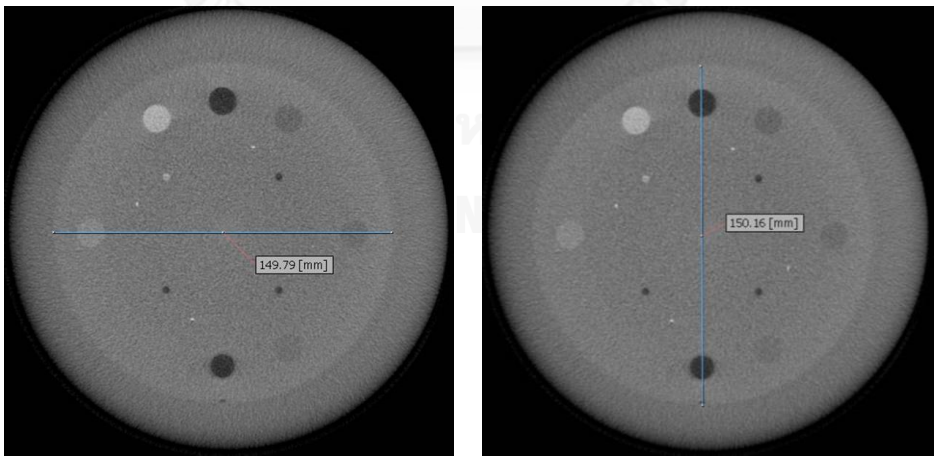

Figure D13: Measurement for diameter distance accuracy in large FOV (FOV20.6x18cm^2)

Table D8: Measured diameter distances, measured distance between Teflon pin and differences between the measured and actual distance

FOV	15x9cm^2		20.6x18cm^2	
Position of distance	Distance (mm)	Different distance	Distance (mm)	Different distance
Diameter of Phantom in x-axis (mm)	149.68	0.32	149.79	0.21
Diameter of Phantom in y-axis (mm)	149.59	0.41	150.16	0.16
Distance between Teflon pin x_1 (mm)	50.13	0.13	49.81	0.19
Distance between Teflon pin x_2 (mm)	50.13	0.13	49.81	0.19
Distance between Teflon pin y_1 (mm)	50.13	0.13	49.94	0.06
Distance between Teflon pin y_2 (mm)	49.89	0.11	50.25	0.25

Remark: Known distance between pin points is 50mm and known diameter is 150mm.

Comment: For both FOVs, images are circular symmetry.

Differences between the measured and actual distance for both FOVs varied from 0.11-0.41mm for FOV 15x9cm^2 and 0.06-0.25mm for FOV 20.6x18cm^2.

PASS

จุฬาลงกรณ์มหาวิทยาลัย
Chulalongkorn University

7. MTF measurement

Purpose: To ensure that the spatial resolution of a reconstructed image comply with manufacturer's standard.

Method: -Place CATPHAN®600 in upright position.

- Acquire an image of section CTP 591 for both FOVs (15x9, 20.6x18cm^2) at 90kVp, 10mA and 10.8seconds.

- Measure MTF by Image J.

Tolerance: - The value of the Modulation Transfer Function (MTF) at 10% is superior to 1 lp/mm.

Results:

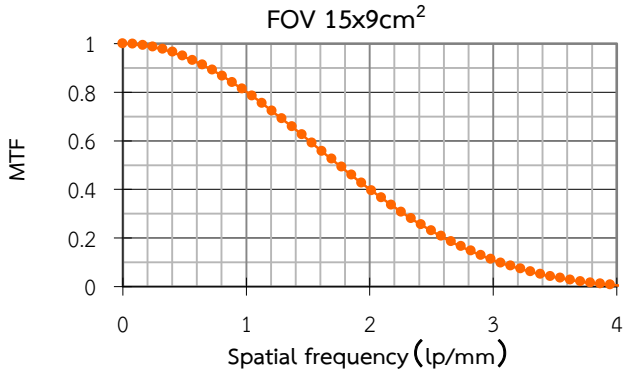

Figure D14: Modulation transfer function vs spatial frequency graph of medium FOV

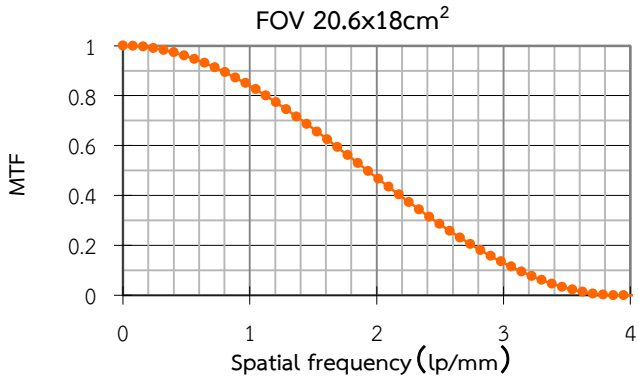

Figure D15: Modulation transfer function vs spatial frequency graph of large FOV

Table D9: Modulation Transfer Function at 10% of medium and large FOV

MTF	Spatial frequency (lp/mm)	
	FOV 15x9cm^2	FOV 20.6x18cm^2
10%	3.0	3.1

Comment: PASS

8. High resolution measurement

Purpose: To visually evaluate the spatial resolution of a reconstructed image.

Method: **-** Place CATPHAN®600 in upright position.

- Acquire an image of section CTP 528 for both FOVs (15x9, 20.6x18cm^2) at 90kVp, 10mA and 10.8seconds.

- Count line pair per centimeter.

a. FOV 15x9cm^2 b. FOV 20.6x18cm^2

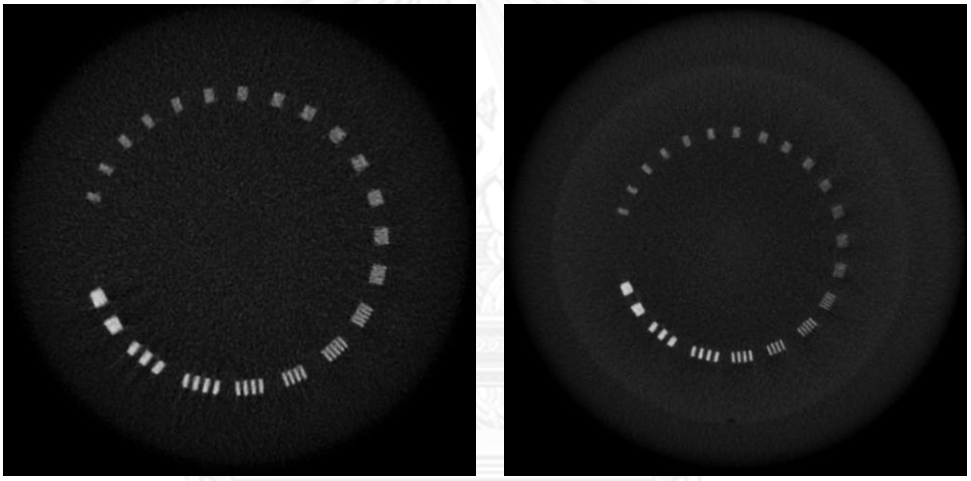

Figure D16: Image of 21 line pairs per centimeter of medium FOV (a) and large FOV (b)

Table D10: Line pair per centimeter of medium and large FOV

FOV	High resolution (lp/cm)	Gap size
FOV 15x9cm^2	7	0.071 cm
FOV 20.6x18cm^2	7	0.071 cm

9. CT number accuracy, noise, uniformity and image artifact

Purpose: CT number and noise values comply with the manufacturer's specifications.

CT number values in homogenous medium are uniform.

Artifacts are not visible.

Method: - Place CATPHAN® 600 in upright position.

- Acquire an image of section CTP 486for both FOVs (15x9, 20.6x18cm^2) at 90kVp, 10mA and 10.8seconds.

- Measure ROI (5cm^2) with eFilm™ software (see figure below).

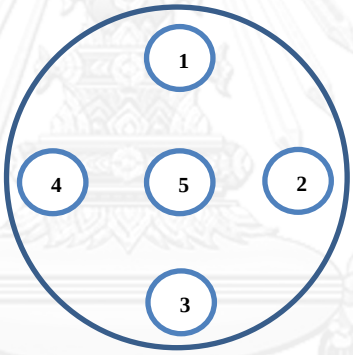

Figure D17: ROI position for measurement

จุฬาลงกรณ์มหาวิทยาลัย
Chulalongkorn University

Tolerance: - CT number is within ±5% from baseline value.

- Image noise is within ±25% from baseline value.

- Difference of CT numbers (measured ROI mean value) between a centrally placed ROI with each of four ROIs placed on the edge should be within ±10 HU

- No artifact in the image.

Results:

CT number accuracy, noise, uniformity

a. FOV 15x9cm^2

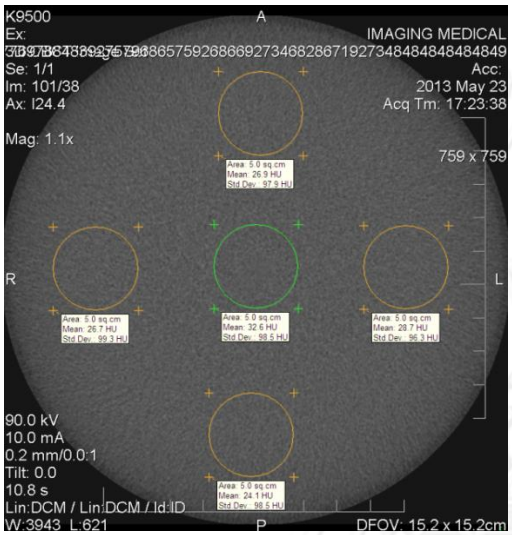

b. FOV 20.6x18cm^2

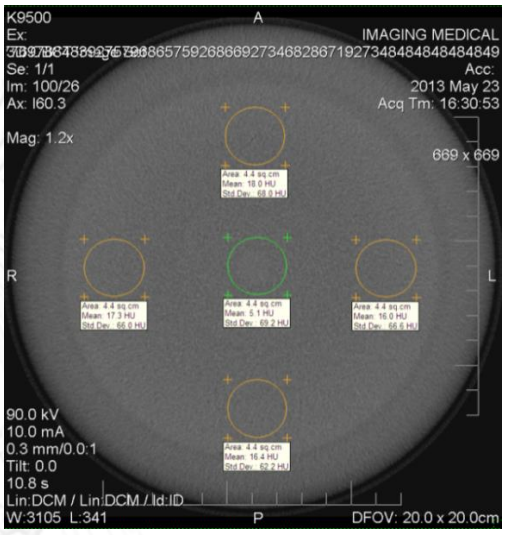

Figure D18: Measurement of 5 ROI in different position. Central ROI used for CT number and image noise; peripheral and central ROI used for uniformity.

Table D11: Mean and SD of ROI values and difference CT number

Position of ROI	FOV 15x9cm^2			FOV 20.6x18cm^2		
	Mean (HU)	SD	Difference CT number	Mean (HU)	SD	Difference CT number
1	26.9	97.9	-5.7	14.8	66.7	9.4
2	28.7	96.3	-3.9	15.2	66.3	9.8
3	24.1	98.5	-8.5	12.7	62.8	7.3
4	26.7	99.3	-5.9	14.9	64.6	9.5
5	32.6	98.5	0	5.4	67.1	0
Average	27.8	98.1		12.6	65.5	

PASS

Image artifact

a. FOV 15x9cm^2 b. FOV 20.6x18cm^2

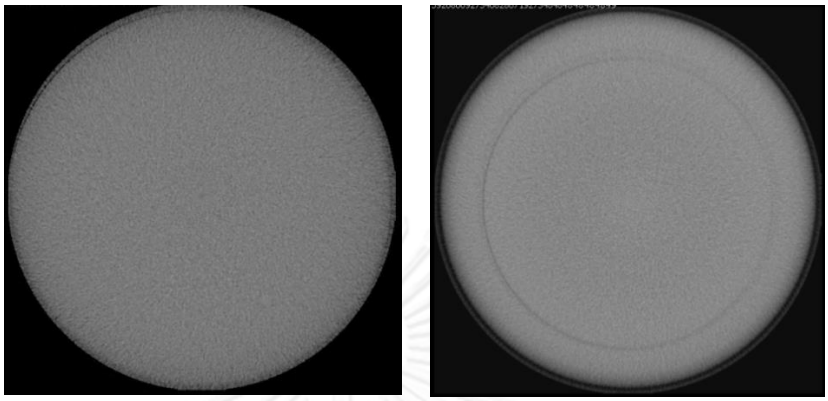

Figure D19: Axial view of phantom section CTP 486 used for inspection of artifact

Comment: FOV 15x9cm^2,

- CT number = 32.6HU and SD = 98.5
- Differences of CT numbers vary from -8.5 to -3.9HU, so the mage is uniformity.
- There is no artifact in the image.

PASS

FOV 20.6x18cm^2

- CT number = 5.4HU and SD = 67.1
- Differences of CT numbers vary from 7.3 to 9.8HU, so the mage is uniformity.
- There is no artifact in the image.

PASS

(CT number and noise cannot compare with manufacturer's specification because it's not available.)

จุฬาลงกรณ์มหาวิทยาลัย
Chulalongkorn University

10. CT number linearity

Purpose: To ensure that the CT number of range of material falls within the required values.

Method: - Place CATPHAN® 600 in upright position.

- Acquire an image of section CTP 404 for both FOVs (15x9, 20.6x18cm^2) at 90kVp, 10mA and 10.8seconds.

- Measure CT number for each material (ROI 0.7cm^2) with eFilm™ software.

Tolerances: -Difference between measured CT number and CT number specified by manufacturer should be within ±20HU

- R-square between measured CT number and linear attenuation coefficient (μ) more than 0.9

Results:

a. FOV 15x9cm^2 b. FOV 20.6x18cm^2

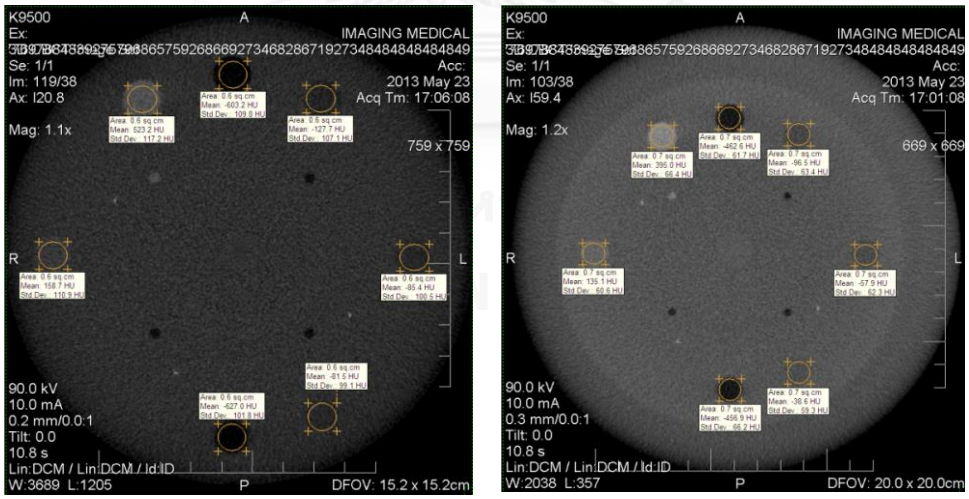

Figure D20: Measurement of CT number for each material of medium FOV (a) and large FOV (b)

Table D12: Difference between estimated and measured CT number

Material	Estimated CT number	FOV 15x9cm^2 Measured CT number	Difference	FOV 20.6x18cm^2 Measured CT number	Difference	Linear attenuation coefficient μ (cm^{-1})
Air1	-1000	-627.0	373.0	-456.9	543.1	0
Air2	-1000	-603.2	396.8	-462.6	537.4	0
PMP	-200	-127.7	72.3	-96.5	103.5	0.25
LDPE	-100	-85.4	14.6	-57.9	42.1	0.277
Polystyrene	-35	-81.5	-46.5	-38.6	-3.6	0.31
Delrin™	340	158.7	-181.3	135.1	-204.9	0.548
Teflon	990	523.2	-466.8	395	-595	1.091

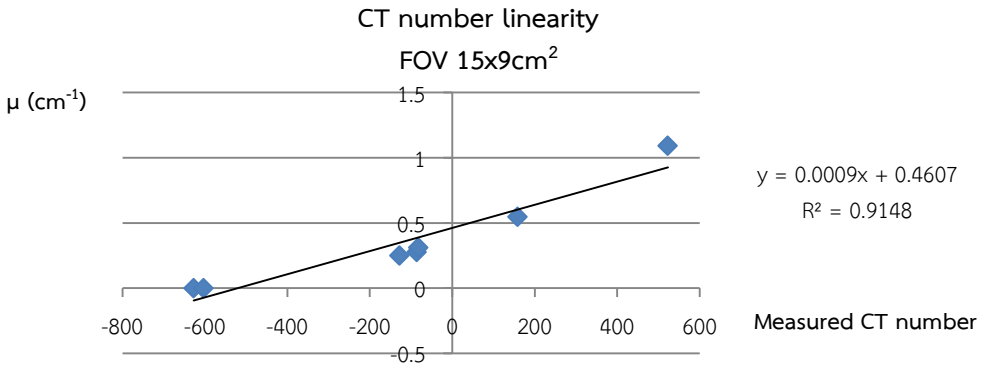

Figure D21: The linearity of CT number with R^2 of 0.9148 of medium FOV

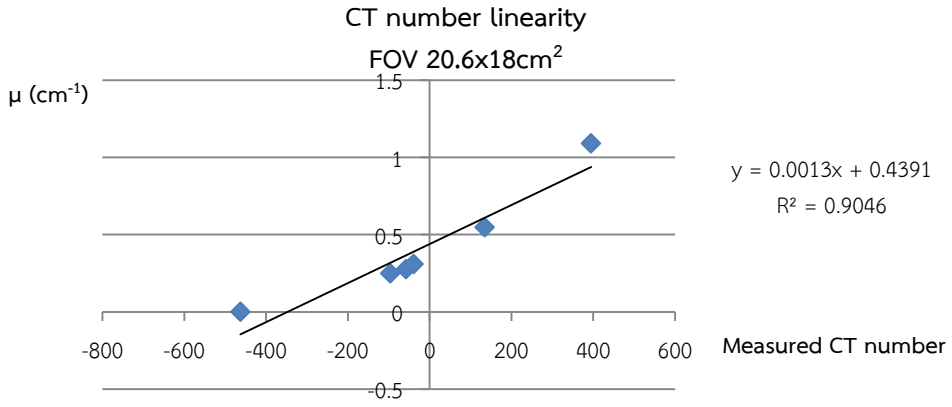

Figure D22: The linearity of CT number with R^2 of 0.9046 of large FOV

Comment: Although R-square between measured CT number and linear attenuation coefficient (μ) for both FOV are more than 0.9 (FOV 15x9cm^2: R^2 =0.9148, FOV 20.6x18cm^2: R^2 =0.9046), differences between measured CT number and CT number specified by manufacturer are more than ±20HU except LDPE (difference = 14.6HU) in FOV 15x9cm^2 and polystyrene (difference = -3.6HU) in FOV 20.6x18cm^2.

CT number in CBCT is inaccuracy.

FAIL

จุฬาลงกรณ์มหาวิทยาลัย
CHULALONGKORN UNIVERSITY

VITA

Name	Miss Warangkana Weerawanich
Date of birth	December 22, 1982
Place of birth	Bangkok, Thailand
Education	Faculty of Dentistry, Mahidol University D.D.S., 2007 Faculty of Dentistry, Mahidol University Higher Graduate Diploma (Dentistry: Oral and Maxillofacial Radiology), 2009

Academic Publications

1. Weerawanich, W. Multiple osteoradionecrosis of jaws: a case report. Thai J Oral Maxillofac Surg 24 (2010): 58-63.

2. Weerawanich, W. and Krisanachinda, A. Effect of field of views on cone beam computed tomography radiation dose: Phantom study. In Proceedings of 13th Asia-Oceania Congress of Medical Physics & 11th South-East Asian Congress of Medical Physics, pp. 113-6. Singapore, 2013.

Current work position and office

Lecturer at Department of Oral and Maxillofacial Radiology, Faculty of Dentistry, Mahidol University. 6 Yothi Rd., Thung Phayathai, Ratchatewi, Bangkok 10400.